# Inter-satellite tracking methods and applications: A comprehensive survey

Jain, R.; Speretta, S.; Dirkx, D.; Gill, E.K.A.

**DOI**
10.1016/j.asr.2024.08.022
10.1016/j.asr.2024.08.022

**Publication date**
2024

**Document Version**
Final published version

**Published in**
Advances in Space Research

**Citation (APA)**
Jain, R., Speretta, S., Dirkx, D., & Gill, E. K. A. (2024). Inter-satellite tracking methods and applications: A comprehensive survey. *Advances in Space Research*, *74*(8), 3877-3901. https://doi.org/10.1016/j.asr.2024.08.022, https://doi.org/10.1016/j.asr.2024.08.022

**Important note**
To cite this publication, please use the final published version (if applicable).
Please check the document version above.

Available online at www.sciencedirect.com

ScienceDirect

Advances in Space Research 74 (2024) 3877–3901

ADVANCES IN SPACE RESEARCH (a COSPAR publication)

www.elsevier.com/locate/asr

# Inter-satellite tracking methods and applications: A comprehensive survey

Rashika Jain *, Stefano Speretta, Dominic Dirkx, Eberhard Gill

*Delft University of Technology, Faculty of Aerospace Engineering, Kluyerweg 1, Delft 2629 HS, the Netherlands*

Received 28 February 2024; received in revised form 19 July 2024; accepted 7 August 2024
Available online 13 August 2024

**Abstract**

The accurate measurement of inter-satellite distances is fundamental to the successful operation of distributed spacecraft missions, facilitating diverse applications ranging from scientific exploration to navigation and communication. This study comprehensively overviews applications requiring inter-satellite tracking by analyzing 44 multi-spacecraft missions. These missions are divided into seven categories based on their use of inter-satellite distance measurements. Each category necessitates varying levels of accuracy, prompting the utilization of distinct tracking methods. The analysis reveals that missions near Earth typically rely on Global Navigation Satellite Systems measurements, achieving millimeter-level accuracy, while lunar missions opt for radio ranging for centimeter-level accuracy. Inter-satellite Laser Ranging Interferometry emerges as the preferred method for missions demanding exceptionally high accuracy (nanometer to picometer range), such as those dedicated to gravitational wave detection and gravimetry. Notably, the analysis identifies a burgeoning trend towards the adoption of Inter-satellite Laser Transponder Ranging, capable of achieving sub-millimeter accuracy. Furthermore, this work proposes a novel concept: integrating inter-satellite ranging with Laser Communication Terminal (LCTs), either to substitute for existing tracking methods or to enhance measurement accuracy within established frameworks. However, its full potential rests upon the successful adaptation of existing LCTs for ranging functionality without compromising data rates. Future research will play a critical role in quantifying achievable ranging performance by characterizing systematic errors within LCTs.


*Keywords:* Inter-satellite tracking; Satellite-to-satellite tracking; Ranging methods; Laser ranging; Data-aided ranging; Free-space optical ranging

## 1. Introduction

In space missions, the involvement of multiple satellites working together can be essential for addressing complex scientific inquiries, studying the intricacies of Earth systems, and advancing technological frontiers. These collaborative missions yield diverse data sets from multiple vantage points, enhancing spatial and temporal resolution. One recurring requirement in many of these missions is the accurate measurement of the relative position of these satellites (Zhang et al., 2022), which is crucial either for enhancing the mission's scientific output or for maintaining its formation.

Two primary methods are used to obtain relative position measurements among satellites: indirect and direct (Turan et al., 2022). The former utilize existing infrastructure like the Global Navigation Satellite Systems (GNSS) and ground-based tracking stations to independently determine the absolute positions of each satellite, which are then mathematically converted to relative positions. However, this approach is constrained by limitations in accuracy and availability due to factors like atmospheric interference, signal attenuation over long distances, and

* Corresponding author.
*E-mail addresses:* r.jain-1@tudelft.nl (R. Jain), s.speretta@tudelft.nl (S. Speretta), d.dirkx@tudelft.nl (D. Dirkx), E.K.A.Gill@tudelft.nl (E. Gill).

https://doi.org/10.1016/j.asr.2024.08.022
0273-1177/

dependence on ground stations. In contrast, direct methods employ dedicated equipment like radio or laser transponders on the satellites for inter-satellite distance measurements, commonly referred to as inter-satellite tracking. This approach offers exceptional accuracy and near-real-time data but increases the mission complexity and cost.

Radio tracking is the most widely used method due to its mature technology and compatibility with existing on-board radio communication systems. A dedicated ranging code phase-modulated and multiplexed with the communication signal facilitates these tracking measurements. However, this approach necessitates the sharing of on-board power between communication and ranging functions, potentially compromising data rate and ranging accuracy (Hamkins et al., 2015).

Laser communication, however, presents a compelling alternative for future space missions. In contrast to radio waves, lasers operate at shorter wavelengths and offer significantly smaller divergence, facilitating higher data rates, enhanced security, and more compact terminals. Consequently, an increasing number of space missions are adopting laser communication technology (Toyoshima, 2021).

The Terabyte Infrared Delivery (TBIRD) program is a noteworthy example, demonstrating a laser downlink at a speed of 200 Gigabits per second (Gbps) from a Low-Earth Orbit (LEO) satellite (Schieler et al., 2022). Historical in-orbit experiments, such as Semiconductor Inter-satellite Link Experiment (SILEX) (Tolker-Nielsen and Oppenhauser, 2002), Lunar Laser Communication Demonstration (LLCD) (Boroson and Robinson, 2014; Stevens et al., 2016), and Short-Range Optical Intersatellite Link (SROIL) (Sodnik et al., 2010), have also utilized lasers for data transfer at speeds ranging from a few Megabits per second (Mbps) to a few Gbps. Furthermore, mega satellite constellations such as Starlink (Brashears, 2024) and Kuiper (Amazon, 2023) have demonstrated inter-satellite laser links with speeds of 100 Gbps, and the upcoming Telesat Lightspeed constellation (Yared and Jansson, 2023) also intends to utilize 10 Gbps laser links for inter-satellite communication.

The advantages of lasers extend beyond communication to offer the potential for more accurate tracking measurements compared to radio. While laser tracking using reflectors is an established technique (Degnan, 1994), its accuracy is limited by atmospheric and reflector response. Therefore, achieving more precise measurements requires a different technology, such as laser transponders. However, unlike radio transponder tracking, multiplexing using lasers requires a more complex system design, necessitating a separate ranging system on each satellite. This requirement increases the Size, Mass and Power (SMaP) consumption and cost of the mission. Thus, if the need for a separate signal for direct range measurements is eliminated, it could mitigate inter-system interference and enhance mission efficiency. Therefore, extensive research is underway in both radio (Andrews et al., 2010; Hamkins et al., 2015; Hamkins et al., 2016a; Hamkins et al., 2016b; Vilnrotter and Hamkins, 2019; Turan et al., 2023) and optical domains (Net and Hamkins, 2020; Net, 2023) to measure the range using communication signals.

While the potential of combined communication and ranging is promising, unlocking their full potential necessitates identifying applications where such technology can be crucial. This paper aims to fill this gap in scientific literature by performing a survey on various applications requiring inter-satellite tracking. By providing an overview of these applications, the paper seeks to assess the potential impact of combined communication and ranging systems. To the authors' knowledge, only one previous survey by Zhang et al. (2022) has focused on inter-satellite measurements. Although the survey thoroughly examined relative state measurement technologies for distributed spacecraft, its focus was limited to identifying methods and associated errors for 15 missions. The current study significantly expands the scope not only by analyzing 44 missions (including 33 not previously examined) but also by categorizing them into various application types. Furthermore, it delves deeper by establishing essential links between specific applications, their corresponding tracking methods, and performance requirements. This survey identifies the applications that necessitate inter-satellite tracking and highlights the prevalent trends observed within the missions. In addition, this work sheds light on the broader potential of combined communication and ranging systems, paving the way for future advancements in the field.

To achieve this objective, past, present, and future missions utilizing inter-satellite tracking are investigated, addressing the following key questions:

> *Which space applications require inter-satellite tracking? What level of precision is needed for tracking in these applications? Which tracking methods are currently employed to meet these requirements?*

Ultimately, the answers to these questions will lead to a more significant inquiry:

> *In which applications can a combined communication and ranging system be critical?*

This paper first details different tracking techniques for measuring inter-satellite distances in Section 2. Then, in Section 3, the past, present, and future missions relying on inter-satellite tracking measurements are analyzed, focusing on the methods used for these measurements. This survey helps identify primary application areas and precision requirements for such missions. Finally, Section 4 provides an analysis highlighting common trends and identifying potential applications for a combined laser communication and ranging system.

## 2. Tracking methods

Tracking methods can be classified into two categories depending upon the type of measurement: range or

range-rate. The former provides the spatial separation between satellites at a specific time, and the latter provides the change in range over a certain integration time. Integration time, the duration over which measurements are combined, plays a crucial role in determining measurement precision. Longer integration times can average out noise, improving precision and signal-to-noise ratio, but may miss rapid changes. The optimal integration time depends on the desired accuracy, signal dynamics, and available processing power. These tracking methods can also be categorized based on the technology used, i.e., radio or laser. Fig. 1 presents the tracking methods and technologies used in space missions.

The term "range/range-rate measurements" does not refer to distance/velocity measurements; rather, it encompasses time, phase, or frequency measurements, depending on the specific tracking method employed.

### 2.1. Range measurements

This subsection dives into various ranging methods employed in space missions. These methods differ based on the type of the signal, the frequency, and the architecture used. Therefore, the following discussion is divided into four parts: ranging signals, ranging frequencies, ranging architectures, and ranging methods.

#### 2.1.1. Ranging signals

Ranging signals exchanged between satellites to determine distance can be broadly categorized into pulsed and continuous wave systems based on their transmission patterns.

i. Pulsed systems transmit short (ns), high-energy (mJ) pulses and measure the time elapsed between transmission and reception of the signal (Degnan, 1985). These systems are particularly effective in long-range applications due to their ability to overcome signal attenuation through high-power transmission. The pulsed nature of the signal aids in distinguishing it from background noise and interference by allowing the receiver to isolate the signal based on its precise timing and high peak power, creating a strong contrast against continuous or random noise. Additionally, the predictable repetition rate of the pulses enables synchronization, further filtering out irrelevant signals. However, the range resolution of the pulsed systems is limited by the pulse width, necessitating a trade-off between resolution and peak power. Shorter pulses provide better resolution but require higher peak power to maintain the same signal strength. Furthermore, the pulse repetition rate is limited by the round-trip travel time to avoid ambiguity from overlapping pulses.

ii. Continuous Wave (CW) systems transmit a continuous electromagnetic wave, with distance measurements derived from analyzing the phase shift or frequency change between the transmitted and received signals (Montenbruck and Gill, 2000, 2013, Chapter 6). These systems provide superior range resolution compared to pulsed systems, as they are not limited by pulse width. However, for distances exceeding the wavelength of the signal, CW systems encounter integer phase ambiguity, which complicates the determination of the absolute distance due to the repeated phase cycles. While CW systems enable precise relative distance measurements, they require more complex signal processing to derive absolute distance. Furthermore, CW systems are more susceptible to continuous background noise, and the continuous transmission results in lower peak power, potentially limiting operational range.

The choice of the signal shape depends on the specific application and mission requirements. Additionally, a continuous wave signal can be modulated to transmit a pulsed signal. However, the quality of such measurements will not be the same as achieved with a dedicated pulsed system and will depend upon the modulation bandwidth available.

#### 2.1.2. Ranging frequencies

Ranging is performed using electromagnetic waves at different frequencies: laser and radio. Each has unique characteristics, advantages, and limitations that make them suitable for specific applications (Kaushal and Kaddoum, 2017).

i. Laser ranging systems operate within the terahertz spectrum (150–600 THz), which offer higher bandwidth compared to Radio Frequency (RF) systems, thereby enabling fine-resolution measurements. The short wavelength (μm-range) inherent to laser technology allows for precise measurements. Additionally, the inherent directionality of laser beams

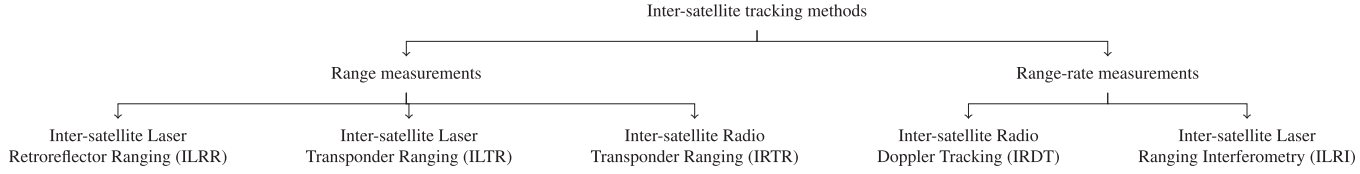


Fig. 1. Inter-satellite tracking methods and technology.

effectively minimizes background noise contamination. While the narrow beam profile enhances security, it also poses stringent pointing requirements, especially when tracking dynamically moving targets. Furthermore, laser signals are highly susceptible to atmospheric scattering, which can significantly degrade performance and compromise tracking accuracy, particularly during adverse weather conditions.

ii. Operating in the 0.3–40 GHz frequency range, RF signals are resilient to atmospheric phenomena, ensuring continuous acquisition of tracking data. Additionally, the broader dispersion of radio waves simplifies pointing requirements compared to laser systems, although this characteristic makes them more susceptible to interception. Nevertheless, the RF technology possesses a well-established foundation in inter-satellite tracking with readily available equipment. However, RF systems require significantly more SMaP compared to laser counterparts, which is a drawback for satellite on-board systems.

### 2.1.3. Ranging architectures

Ranging architecture refers to how the ranging signals are exchanged between the satellites. Fig. 2 depicts four prevalent architectures used for range measurements, and Eq. (1) shows how to compute range ($R$) using the Time of Flight (TOF) method for each architecture.

$$R = \begin{cases} c \cdot (t_2^B - t_1^A) = c \cdot (t_2^A - t_1^A + \tau), & \text{OWR} \\ c \cdot [(t_2^B - t_1^A) + (t_2^A - t_1^B)]/2 = c \cdot [(t_2^A - t_1^A) + (t_2^B - t_1^B)]/2, & \text{STWR/ATWR} \\ c \cdot (t_2^A - t_1^A)/2, & \text{TWRR.} \end{cases} \tag{1}$$

The following notations will be used in this section: $A$ and $B$ represent the two satellites, $T_x$ and $R_x$ are the transmitter and receiver, $t^i$ represents the time measured by the satellite $i$ clock, $t_1^i$ and $t_2^i$ are the transmission and reception times, respectively, and $\tau$ is the clock offset between $A$ and $B$. The time at which $R$ is measured can be either $t_2^A$ or $t_2^B$ and depends on the realization of the system.

i. **One-Way Ranging (OWR)**: In Fig. 2a, a signal is transmitted from satellite $A$ and received on satellite $B$. Since measurements are done on different satellites and depend on precise time-of-flight, the on-board clocks must be precisely synchronized. This is the main reason why OWR is less preferred.

ii. **Two-Way Ranging (TWR)**: The synchronization challenge is overcome by introducing a return signal that cancels out the clock offsets. Depending on how the return signal is transmitted, TWR has four variations:

   a. **Synchronous Two-Way Ranging (STWR):** When the second satellite is also equipped with a transponder, as shown in Fig. 2b, which receives, amplifies, and retransmits the signals, the technique is called STWR. As both satellites take time measurements, the clock offset is canceled in the final range computation (please refer to Eq. (1)). It should be noted that instead of time-tagging the signals on $B$, the quantity $\Delta t = (t_1^B - t_2^B)$, also called transponder delay, is recorded on $B$ and transmitted to $A$ using the communication link. Since $B$ always waits for a signal from $A$, $\Delta t$ is always a positive value.

   b. **Asynchronous Two-Way Ranging (ATWR):** If both satellites transmit signals simultaneously, as in Fig. 2c, this is defined ATWR: more range measurements can be taken in the same duration, as compared to STWR. The time tags are exchanged between satellites using an alternative communication link and the two-way range is computed by pairing the range measurements from the two

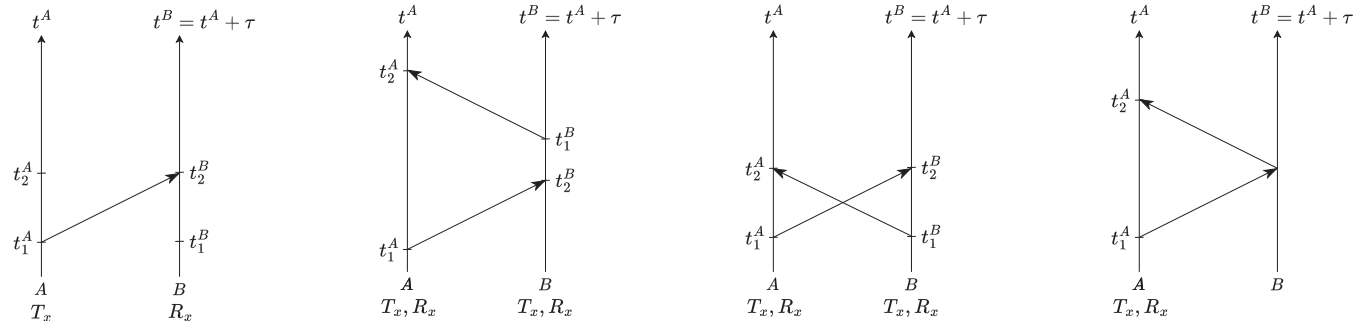


(a) One-Way Ranging (OWR) (b) Synchronous Two-Way Ranging (STWR) (c) Asynchronous Two-Way Ranging (ATWR) (d) Two-Way Retro-reflector Ranging (TWRR)

Fig. 2. Schematic of various ranging architectures. A and B represent the two satellites. $T_x$ is the transmitter, and $R_x$ is the receiver. $t^A$ and $t^B$ represent the time measured by clocks of A and B, respectively. The subscripts 1 and 2 stand for transmission and reception time, respectively. $\tau$ is the offset between the two clocks.

satellites. However, it requires signal pairing techniques to resolve the ambiguity created by simultaneous transmissions, i.e., pairing the correct transmitted signal from $B$ to the transmitted signal from $A$ (Dirkx, 2015, Chapter 3).

c. **Two-Way Retro-reflector Ranging (TWRR):** If the second satellite acts as a passive node, as shown in Fig. 2d, the configuration is defined TWRR: both the transmitter and receiver are placed on a single satellite, and the transmitted signal reflects off the other satellite using retro-reflectors, eliminating the need for two clocks. However, in this configuration, the same signal experiences Free-Space Loss (FSL) twice, leading to low Signal-to-Noise Ratio (SNR) at the receiver. The one-way FSL is directly proportional to the square of the distance ($\sim d^2$), and upon reflection, it becomes proportional to the fourth power of the distance ($\sim d^4$). Consequently, as the distance between the transmitter and the receiver increases, the SNR at the receiver rapidly decreases, making this approach typically impractical for longer distances. Satellite Laser Ranging (SLR) (Degnan, 1994) uses pulsed-TOF TWRR for ground-based tracking of satellites, but it is limited to lunar distances.

d. **Dual One-Way Ranging (DOWR):** In the radio domain, range measurements done using two-way transponder-based architectures are also referred to as DOWR. Instead of time-based measurements, DOWR typically relies on dual one-way phase measurements to determine the inter-satellite range. Each transmitted signal carries reference phase information, and the receiver detects the phase shift relative to its reference phase. The measured phase shifts and the arrival time-tags are exchanged between satellites using a communication link. The dual one-way range, $R(t)$, is then computed using Eq. (2) (Kim, 2000).

$$R = c \cdot \frac{\varphi_A(t_2^A) + \varphi_B(t_2^B)}{f_A + f_B}, \tag{2}$$

where $A$ and $B$ represent the two satellites, $\varphi_i(t)$ represents the differential phase measurement at satellite $i$ at reception time $t$, $c$ is the velocity of light and $f_i$ is the frequency of the transmitted signal from satellite $i$.

The discussed ranging architectures are adaptable to various inter-satellite ranging methods. However, two-way measurements are typically preferred over one-way measurements since they are not affected by the absolute clock differences between the different satellites. Nevertheless, for all two-way architectures except TWRR, the exchange of time tags over a communication link is necessary to facilitate range measurements.

#### 2.1.4. Ranging methods

In principle, range measurements can be taken using any combination of signal shape, frequency, and architecture. However, in practical applications, three methods are commonly employed for inter-satellite ranging (refer to Fig. 1). Each method discussed in this sectionpossesses unique characteristics that determine its suitability for specific mission requirements.

i. **Inter-satellite Radio Transponder Ranging (IRTR)**: This method primary utilizes DOWR measurements with radio transponders on both satellites. The wider beamwidth of radio signals facilitates link establishment without stringent pointing accuracy. However, a significant drawback is the susceptibility of radio signals to ionospheric delay, necessitating dual-frequency measurements for accurate correction (Kim, 2000). Additionally, radio transponders are larger in size compared to their laser counterparts, potentially posing challenges for missions with limited SMaP availability.

ii. **Inter-satellite Laser Retro-reflector Ranging (ILRR)**: ILRR employs TWRR, which does not require time-tag exchange as the second satellite functions passively. While this method reduces system complexity and SMaP requirements, the ranging signal experiences significantly higher attenuation compared to other methods, limiting ILRR's applicability to missions involving large inter-satellite distances.

iii. **Inter-satellite Laser Transponder Ranging (ILTR)**: ILTR can employ any of the OWR, STWR or ATWR architectures based on mission requirements along with a separate link to exchange time-tags between the satellites. This method provides a better alternative for ranging measurements than the previous ones, leveraging the high-precision laser technology while mitigating signal loss compared to ILRR. However, the narrower divergence of the laser beam necessitates precise pointing for establishing the link. Traditionally, ILTR systems use encoded laser signals for range measurements, as exemplified by cm-order measurements by Lunar Laser Communication Demonstration (LLCD) (Boroson and Robinson, 2014). However, recent advancements have demonstrated the potential of phase-based measurements for obtaining range information with even higher precision (Giorgi et al., 2019).

The maturity of radio technology has established IRTR as the prevalent method for direct inter-satellite ranging. However, the emergence of LCTs capable of ILTR presents a promising avenue for achieving high-precision measurements. A recent study by Grenfell (2024) has demonstrated the potential for millimeter-order range precision using LCTs. Nevertheless, laser-based technologies are still in the development phase, necessitating further

research to quantify potential errors and establish achievable performance metrics.

### 2.2. Range-rate measurements

This subsection covers tracking methods for determining range-rate, i.e., change in range over a certain integration time. Two techniques used to extract range-rate information are Inter-satellite Radio Doppler Tracking (IRDT) and Inter-satellite Laser Ranging Interferometry (ILRI).

#### 2.2.1. Doppler tracking

The IRDT technique utilizes the Doppler effect, where the frequency of a signal changes due to relative motion between the transmitter and receiver. When a signal is transmitted from one satellite to another, the received signal exhibits a Doppler shift. This shift, measured as the difference between the received frequency and the reference frequency, serves as the basis for computing the integrated range-rate, as given in Eq. (3):

$$\dot{\rho} \approx c \cdot \frac{\Delta f}{f_T}, \tag{3}$$

where $\dot{\rho}$ is the integrated range-rate, $\Delta f$ is the Doppler shift and $f_T$ is the frequency of the transmitted signal. While Eq. (3) provides a first-order approximation, a complete derivation can be found in Turyshev et al. (2013) and Bocanegra-Bahamón et al. (2018). Notably, the accuracy of these range-rate measurements crucially depends on the accuracy of the reference frequency. As oscillator stability is susceptible to factors like temperature and aging, even minor errors in the reference frequency can propagate to significant range-rate uncertainties.

#### 2.2.2. Interferometric tracking

ILRI uses the properties of an interferometer to determine the precise relative displacement of satellites using lasers. A laser beam is reflected off the mirrors placed on the satellites, and the interference pattern formed by the reflected beams is measured. When external forces, such as a gravitational pull from a celestial body, act upon either of the satellites, it changes the distance between them. This change affects the arm length of the interferometer, causing either a delay or advancement in the reflected signal, leading to a shift in the interference pattern. Therefore, ILRI monitors the change in interference by measuring the signal's phase shift with respect to a reference. The variation in the arm length of the interferometer or the separation between the satellites ($\Delta L$) can be computed using Eq. (4) (Kim et al., 2020),

$$\Delta L = \lambda \cdot \Delta\varphi, \tag{4}$$

where $\lambda$ is the wavelength of the transmitted signal and $\Delta\varphi$ is the phase shift measured in cycles.

### 2.3. Indirect measurements

The methods discussed in Section 2.1,2.2 provide the range/range-rate by taking direct measurements between two satellites. Alternatively, distance can also be computed indirectly without the exchange of ranging signals. This method relies on the absolute position vectors of both satellites, which can be obtained from various sources such as GNSS-measurements, or ground-based tracking systems. In this survey, only the former is included as it does not depend on ground systems to provide real-time position information. However, it is important to note that satellites in the GNSS network still rely on ground systems for orbit maintenance and clock synchronization (Teunissen and Montenbruck, 2017).

### 2.4. Measurement errors

All inter-satellite tracking measurements are susceptible to deviations from the true range, resulting in measurement errors. These deviations can be categorized into two types: systematic errors and random noise. Systematic errors introduce consistent biases in the measurements, either constant or time-varying. The former can be corrected through calibration (on the ground or in orbit) or post-processing techniques, while the latter requires modeling techniques. Common systematic errors include instrumental delays, pointing errors due to satellite attitude or vibrations, center-of-mass offsets, attitude control, and knowledge errors. In one-way range architectures, the time-variability of the clock biases induces a time-variable range bias, which degrades the quality of the measurements (Dirkx et al., 2015).

Random noise, arising from various sources such as time-tagging electronics and signal detection, introduces uncertainty in measurements. While these sources cannot be entirely eliminated, they can be statistically modeled to assess their impact on overall measurement uncertainty. However, limitations in the noise quantification models compared to real-world dynamics can introduce additional uncertainties. The important challenges in accurately characterizing random noise include the time-correlation of random noise levels and the accurate determination of the noise probability distribution function.

The specific error sources can vary depending on the inter-satellite tracking method employed. Common error sources in IRTR include multipath errors (where the signal reaches the receiver via multiple paths), attitude control and knowledge errors, thermal variations within the instruments, oscillator noise, time-tag errors, and delays introduced by the transponders used in the ranging process (Bertone et al., 2018; Kim and Lee, 2009). On the other hand, preliminary research by Grenfell (2024) suggests that clocks, event timers, and detectors are the main sources of errors in ILTR. However, it is a relatively new method, and

further research is required to gain a detailed understanding of the specific error characteristics of ILTR systems. No missions have yet implemented ILRR, so dedicated studies on its error sources are not currently available. However, based on its similarities to SLR with the exception of atmospheric errors, the main sources of measurement errors are expected to be detector uncertainty, finite laser pulse length, hardware imperfections (including electronic noise and wear-and-tear degradation), and system instabilities like clock and event timer fluctuations (Dirkx et al., 2019).

The performance of tracking measurements is commonly assessed through two key terms: *accuracy* and *precision*. In this paper, accuracy is defined as the systematic errors, while precision refers to the random noise present in measurements. It is essential to differentiate between these two concepts as they are frequently used interchangeably in the literature, making it challenging to create a consistent framework across multiple missions and tracking techniques. Since the true distance between two satellites is not known, a quantification of accuracy is an estimate of the real value. The precision of a dataset can be quantified from its random spread around a mean trend. Therefore, precision will be used as the metric for the comparative analysis in this survey. Additionally, unless explicitly stated otherwise, the ambiguous information provided in the literature is considered to represent precision.

## 3. Applications

This section comprehensively examines past, present, and proposed future missions that employ inter-satellite tracking. Based on the usage of inter-satellite measurements, these missions are divided into seven categories: gravimetry, gravitational wave detection, satellite-based navigation, Earth observation, constellation control, space exploration, and technology demonstration. A total of 44 missions across these categories are discussed in Sections 3.1–3.7, with a particular focus on the employed tracking methods and their corresponding accuracy requirements. Furthermore, the analysis of these missions is consolidated in Section 4 to identify applications where LCTs could provide equivalent or enhanced performance compared to existing inter-satellite tracking methods.

### 3.1. Satellite gravimetry

The non-uniform distribution of mass within celestial bodies leads to variations in their gravitational fields. These variations, further influenced by dynamic mass redistributions such as melting ice caps, affect the motion of orbiting objects. Satellite gravimetry is a technique used to measure subtle changes in a satellite's orbit and reconstruct the underlying gravitational field responsible for these deviations.

Single-satellite missions, such as Challenging Minisatellite Payload (CHAMP) (Reigber et al., 1999) and Gravity Field and Steady-State Ocean Circulation Explorer (GOCE) (Floberghagen et al., 2011), utilized precise positioning data obtained from GNSS receivers and ground tracking to determine the satellite's trajectory. On-board accelerometers account for non-gravitational accelerations, such as atmospheric drag. By removing these effects and comparing the observed trajectory to the predicted orbit, the variations caused by the body's gravitational field can be inferred. While single satellites provide data on the static gravity field, measuring the change in distance between multiple satellites over time allows the mapping of temporal variations in the gravity field, revealing mass movements like water flow or atmospheric changes. Moreover, an inter-satellite link contains significant information about the medium to short wavelength components of the gravitational field (Flechtner et al., 2021). In addition, different harmonics of the gravitational field can be determined by varying the inter-satellite distance, altitude, and configuration of satellite formations. This section discusses satellite missions that employ inter-satellite tracking for gravimetry of Earth and other celestial bodies.

#### 3.1.1. GRACE

The Gravity Recovery And Climate Experiment (GRACE) satellites measured the static gravitational field of Earth and its temporal variations from 2002–2017. The primary goal of the mission was to illustrate the distribution of mass within Earth and its changes over time, making it an essential tool for studying Earth's ocean, geology, and climate.

The mission consisted of an along-track formation of two satellites with a separation of about 220 km in the same low-Earth orbit. One of the significant components of the satellites was the High-Accuracy Inter-Satellite Ranging System (HAIRS). It contained the dual frequency MicroWave ranging Instrument (MWI), more commonly known as the K-Band Ranging (KBR) system, which performed dual one-way carrier phase measurements using microwaves in the K (24 GHz) and Ka (32 GHz) frequency bands (Flechtner et al., 2021), which are converted to DOWR as given in Eq. (2). The KBR can provide micrometer-order ranging accuracy and up to 0.4 μm ranging precision when averaged over 5 s intervals (Kim and Lee, 2009; Tapley, 2008).

Time tags required for DOWR measurements are provided by the on-board GPS receiver and then post-processed on the ground to achieve an accuracy of better than 100 ps (Kim and Lee, 2009).

#### 3.1.2. GRACE-FO

Following the conclusion of the GRACE mission in 2017 due to battery aging, the successor mission GRACE Follow-On (GRACE-FO) was launched in 2018 to continue its legacy. In addition to the proven KBR system for precise inter-satellite ranging, the follow-on mission carries a Laser Ranging Interferometer (LRI) as a technology demonstrator (Heinzel et al., 2017). The LRI employs

standard 1064 nm lasers with 25 mW output power on one satellite and a phase-locked amplifying transponder on the second. The smaller wavelength of LRI ($10^{-4}$ times that of KBR) allows inter-satellite ranging with nanometer-order precision averaged over 2 s integration times, which is two orders of magnitude better than KBR (Darbeheshti et al., 2017). Although the ranging accuracy of GRACE-FO remains at the micrometer-order, the enhanced precision of LRI will allow the measurement of subtle mass changes and an improved spatial resolution for the geopotential model (Sheard et al., 2012).

#### 3.1.3. MAGIC

The Mass-change And Geosciences International Constellation (MAGIC) mission, scheduled for launch in 2028, is a collaborative venture between National Aeronautics and Space Administration (NASA) and European Space Agency (ESA). It builds upon the research conducted by NASA 's Mass Change Designated Observable (MCDO) (Wiese et al., 2022) and ESA 's Next Generation Gravity Mission (NGGM) missions (Haagmans et al., 2020), serving as a successor to the GRACE and GRACE-FO missions. The primary constraint of the GRACE missions is their 30-day integration time in generating gravity maps, which restricts the ability to forecast extreme events such as earthquakes, droughts, and floods. Therefore, the key objective of MAGIC is measuring fluctuations in the gravitational field of Earth at temporal and spatial resolutions better than 1 week and 25 $km^2$, respectively. MAGIC will consist of two pairs of satellites in a Bender constellation: one pair at 89° and another at 69° of inclination (Bender et al., 2008). Each satellite pair will form an Along-track Orbit (ATO) configuration with a separation of 100 km. The two different inclinations allow the observation of the entire signal, including high-frequency components, which could not be done with GRACE-FO. It will reduce the need for extensive post-processing and enable near real-time gravity analysis with an integration time of 5–7 days. MAGIC will carry similar instruments to GRACE-FO, the KBR, and the LRI, and the accuracy of inter-satellite distance change required to meet mission objectives will need to be as little as few nanometers with a sampling rate less than 1 s (ESA Earth and Mission Science Division, 2020).

#### 3.1.4. GRAIL

Inspired by the success of the GRACE mission, the Gravity Recovery and Interior Laboratory (GRAIL) mission was launched in 2011 to recover the Moon's gravity field precisely. The mission involved deploying two identical satellites in a low-altitude, near-circular, polar orbit separated by a distance of 175–225 km. Each satellite was equipped with the Lunar Gravity Ranging System (LGRS) instrument, specifically designed for DOWR (refer to Item ii.) to measure the inter-satellite range-rate (Hoffman, 2009). Compared to the KBR used in GRACE, LGRS had two key distinctions. Firstly, the GRAIL satellites operated outside the Earth's atmosphere, eliminating the need to compensate for ionospheric noise; therefore, the K-band link was removed. Secondly, lacking access to GNSS time-tagging, the GRAIL satellites incorporated an S-band Time Transfer System (TTS) operating at 2 GHz. The absolute timing accuracy after post-processing was found to be 1 μs (Oudrhiri et al., 2014). The range-rate measured by LGRS had an accuracy near 0.03 μm/s at an integration time of 5 s (Konopliv et al., 2013) and a precision of micrometer-order (Klipstein et al., 2013).

#### 3.1.5. Hera

Hera will be launched in October 2024 to study the impact of Double Asteroid Redirection Test (DART) (Rivkin and Cheng, 2023) on Dimorphos - the orbiting Moonlet in the binary asteroid system known as Didymos. Hera, along with its two CubeSats *Juventas* and *Milani*, will characterize the mass and mass distribution of Didymos and Dimporphos using radio science. The variation in Hera's trajectory will be used to reconstruct the gravity field of the asteroid system. Hera will perform two-way Doppler measurements from an Earth-based communication link in the X-band. In addition, it will also have direct Inter-Satellite Links (ISLs) with both daughter CubeSats. The mothercraft will transmit signals operating at S-band frequencies (~2.2 GHz) and collect the CubeSats' telemetry data and measurements, while the CubeSats will act as a transponder (Gramigna et al., 2022). The measured Doppler shift of the ISL contains information about the system's gravity as the CubeSats fly at lower altitudes than the main spacecraft. The accuracy of range and range-rate measured using the ISL for navigation purposes is expected to be better than 50 cm and 0.05 mm/s at 60 s integration time, respectively, with the major limiting factors being the frequency stability of the ISL and thermal noise (Gramigna et al., 2024).

#### 3.1.6. SAGM

The Space Advanced Gravity Measurements (SAGM) is a Chinese mission currently under study. It aims to measure the Earth's gravitational field using Low-Low Satellite-to-Satellite Tracking (LL-SST), like GRACE. A transponder-type laser ranging interferometer system with heterodyne optical phase-locking will be used, like the one for LISA-Pathfinder. An inter-satellite distance of 100–200 km is expected to be measured with nm-order precision (Zhang et al., 2018).

#### 3.1.7. MOBILE

The Mass Variation Observing System by High Low Inter-satellite Links (MOBILE) mission was submitted as a response to the ESA Earth Explorer 10 call. Although the study was considered to be of high scientific merit, the proposal was not selected (Pail et al., 2019).

Nevertheless, the objective of MOBILE was to measure the Earth's temporal gravity and mass variations by observing the distance between Medium-Earth Orbit (MEO) (altitude 10000 km) and LEO satellites (altitude 350–400 km). It was proposed that the LEO satellites will carry a highly-accurate (μm-level) ILRI instrument and perform ranging to the MEO satellites, which act as passive nodes. Therefore, MEO satellites can also be a part of another mission as long as they are equipped with retroreflectors. The advantage of using such high-low links is that the radial component of gravity-induced orbit perturbations can be observed, unlike the low-low links of GRACE missions. It could improve the gravity field performance by a factor of five compared to GRACE-FO, especially in the long wavelengths where the largest amplitudes of time-variable gravity field signals occur (Pail et al., 2019).

### 3.1.8. MAGIA

Missione Altimetrica Gravimetrica geochImica lunAre (MAGIA) is a mission concept which was submitted to Italian Space Agency (ASI) Small Satellites call in 2007. The idea was to measure the gravity of the Moon by using a formation of two co-orbiting small satellites in a lunar orbit at 70 km altitude with a separation of 40–70 km (Perrotta et al., 2010). The mission proposed using S-band signals at 3 GHz to perform Doppler measurements between the two spacecraft. This would have resulted in a range-rate accuracy of 0.1 mm/s at 10 s integration time, leading to a range accuracy of 1 mm (Fermi et al., 2010; Garattini et al., 2012).

### 3.1.9. MARS-SST

The Mars Satellite-to-Satellite Tracking (Mars-SST) mission is proposed to accurately map the static and temporal gravity field of Mars using a pair of satellites with a distance of 40–60 km. The inter-satellite range-rate will be measured using the same laser interferometer as GRACE-FO, and the orbital position of both satellites will be determined using the Deep Space Network (DSN). The range-rate accuracy required to improve the Martian gravitational field model is 100 nm/s (Zheng and Li, 2018).

### 3.1.10. Summary

This section explored the application of inter-satellite tracking in mapping celestial gravitational fields. This technique leverages the precise measurement of minute changes in the distance between co-orbiting satellites to reconstruct the underlying gravitational field of the celestial body they orbit. Missions like GRACE and its successor have successfully employed this approach to create detailed maps of Earth's gravity field, providing valuable insights into mass redistributions and their impact on various geophysical phenomena. The next generation mission, MAGIC, aims to further enhance the resolution and processing speed of these maps by utilizing constellations of four or more satellites. While the MOBILE mission ultimately did not progress beyond the conceptual stage, it introduced the innovative concept of high-low satellite tracking. This approach can measure the radial component of the time-varying gravitational field, a capability not achievable with traditional low-low satellite formations.

The past missions depended majorly upon radio ranging or radio Doppler tracking measurements. However, after the technology demonstration of GRACE-FO, laser-based tracking is being considered for future missions. In the context of low-low links of GRACE-FO, LRI measurements improved the gravity field measurements by one order of magnitude as compared to KBR, especially at higher harmonics where radio signals are dominated by noise (Ghobadi-Far et al., 2020).

The application of inter-satellite tracking extends beyond Earth's orbit. Future missions leveraging this technique are planned to map the gravitational fields of celestial bodies like Didymos and Mars, offering new avenues for understanding their internal structure and mass distribution (Table 1).

Table 1
An overview of the tracking instruments utilized and precision required for satellite gravimetry missions.

| Mission | Year | Orbit/ Configuration | Inter-satellite distance | Inter-satellite measurements | Measurement error | Integration time |
|---|---|---|---|---|---|---|
| GRACE | 2002–2017 | LEO: 2, ATO | 220 km | IRTR K/Ka-band | Range: μm-level | 5 s |
| GRACE-FO | 2018 | LEO: 2, ATO | 220 km | IRTR K/Ka-band, ILRI 1064 nm | Range: μm-level, Range-rate: nm/s-level | 5 s, 2 s |
| SAGM | under study | LEO: 2 | 100–200 km | ILRI 1064 nm | Range: nm-level | – |
| MAGIC | 2028 | LEO: 4, Bender | 100 km | IRTR K/Ka-band | Range-rate: nm/s-level | 1 s |
| MOBILE | cancelled | LEO/ MEO | – | ILRI 1064 nm | Range: μm-level | – |
| GRAIL | 2011–2012 | Moon: 2, ATO | 175–225 km | IRTR Ka-band | Range-rate: 0.03 μm/s | 5 s |
| MAGIA | unknown | Moon: 2, ATO | 40–70 km | IRDT S-band | Range-rate: 0.1 mm/s | 10 s |
| Hera | 2024 | Didymos: 3 | 15 km | IRDT S-band | Range-rate: 0.05 mm/s | 60 s |
| MARS-SST | proposed | Mars: 2, ATO | 40–60 km | ILRI 1064 nm | Range-rate: 0.1 μm/s | 5 s |

### 3.2. Gravitational wave detection

Gravitational waves, tiny ripples in spacetime caused by accelerating masses or cosmic collisions, travel away from the source at the speed of light, causing a minute distortion in the geometry of spacetime that affects everything along their path. One of the ways to detect these waves is by measuring the minute changes in optical path length of laser interferometers (Seto et al., 2001). While ground-based observatories like Laser Interferometer Gravitational-wave Observatory (LIGO) have achieved groundbreaking success in capturing gravitational waves, they cannot go below 10 Hz due to limitations from seismic and gravitational gradient noise (Ming et al., 2020). Since seismic waves are not present in space, upcoming missions are creating space-based interferometers to detect low-frequency gravitational waves.

A key aspect of space-based detection involves precisely measuring the change in the signal's phase with respect to the transmitted laser beam. This phase shift arises because a gravitational wave will change the distance between the satellites. Therefore, the accuracy of wave detection is highly dependent upon the precise measurement of this phase shift. Two future space interferometers are discussed in this section.

#### 3.2.1. LISA

The Laser Interferometer Space Antenna (LISA) mission, scheduled to launch in 2037, will act as an observatory in space to detect and measure gravitational waves in the 0.1–100 mHz range (Amaro-Seoane et al., 2017). LISA will comprise three spacecraft arranged in a triangle formation separated by 2.5 million km in a heliocentric orbit about 50 million km from Earth. Each spacecraft will have two optical assemblies (laser, telescope, test mass) pointing toward the other two. They form a Michelson-type interferometer, with the only difference being that the lasers operate in a transponder mode instead of direct reflection. The test masses are maintained in free-fall inside the spacecraft so that they only experience gravitational forces. A passing gravitational wave will lead to a movement in the test masses and consequently shrink or expand the arm length of the interferometer. These distance variations occur at a timescale of 1000 s and will be measured with picometer-level accuracy by heterodyne interferometry using lasers operating at 1064 nm and delivering 2 W output power (Amaro-Seoane et al., 2017; Yao et al., 2021). The mission also requires an accuracy of better than 1 m in one-way measurements of absolute arm length, measured using inter-satellite laser dual one-way ranging (Yao et al., 2021; Esteban et al., 2011).

Originally, LISA was a joint venture between v and ESA. However, when the former pulled out in 2011, the mission was modified and renamed to evolved-Laser Interferometer Space Antenna (eLISA).

#### 3.2.2. DECIGO

The DECi-Hertz Interferometer Gravitational wave Observatory (DECIGO) is a Japanese project that aims to study gravitational waves in the frequency gap between LISA and terrestrial detectors, 0.1–10 Hz (Musha, 2017). Just like LISA, DECIGO also uses a three-spacecraft configuration in an equilateral triangle in heliocentric orbit. However, each arm length is 1000 km and is measured using a Fabry–Perot interferometer. The lasers used in the interferometer operate at a wavelength of 515 nm with an output power of 10 W (Musha, 2017). DECIGO is planned for launch in the mid-2030s, and the final constellation will consist of four clusters with three satellites each. The mission requirements do not yet provide a specific value for range accuracy. However, ground tests performed with a few kilometers of fiber spool and 1550 nm laser gave a ranging resolution of 6.25 m (Musha et al., 2021).

Another mission called B-DECIGO will be launched in the early 2030s to test the technology for DECIGO. The precursor will have only one cluster of satellites with an arm length of 100 km and lasers yielding 1 W output power (Musha, 2017).

#### 3.2.3. Summary

This section explored two future space-based gravitational wave observatories. Gravitational waves cause minute changes in the distance between satellites, requiring highly precise interferometers capable of detecting picometer-scale variations. The missions, with their different arm lengths, will target distinct frequency ranges for gravitational waves. As shown in Table 2, higher arm lengths allow the detection of lower frequency (longer wavelength) components. The science return is limited by photon shot noise at higher frequencies, as fewer photons can be collected, leading to a lower signal-to-noise ratio. At lower frequencies, the acceleration noise of the test masses, caused by tiny vibrations in their motion, becomes the dominant limitation. Since DECIGO has a shorter arm length and detects higher frequency waves, it uses a high-power laser and Fabry–Perot cavity to overcome shot noise limitation (Musha, 2017). In addition, by comparing the signals from multiple clusters, DECIGO can effectively filter out noise and enhance the true gravitational wave signal.

For completeness, Table 2 also includes two Chinese missions, Taiji (Luo et al., 2021) and TianQin (Mei et al.,

Table 2
An overview of space missions utilizing inter-satellite tracking for gravitational wave detection. The last two missions are explained in Zhang et al. (2022) and are included here for completeness.

| Mission | Year | Orbit/ Configuration | Arm length | Interferometer specifications | Detection frequency | Inter-satellite measurements | Measurement error |
|---|---|---|---|---|---|---|---|
| DECIGO | mid-2030s | Heliocentric: 12 (4 clusters of equilateral triangles) | 1000 km | Fabry–Perot, 515 nm, 10 W | 0.1–10 Hz | ILRI 515 nm | – |
| B-DECIGO | early-2030s | Heliocentric: 3 (equilateral triangle) | 100 km | Fabry–Perot, 515 nm, 1 W | 0.1–10 Hz | ILRI 515 nm | – |
| LISA | 2037 | Heliocentric: 3 (equilateral triangle) | $2.5 \times 10^6$ km | Michelson-type, 1064 nm, 2 W | 0.1–100 mHz | ILRI + ILTR 1064 nm | Change in distance: pm (1000 s time scale), Range: 1 m |
| Taiji | 2030s | Heliocentric: 3 (equilateral triangle) | $3 \times 10^6$ km | Michelson-type, 1064 nm, 3 W | 0.1 mHz–1 Hz | ILRI 1064 nm | Change in distance: pm |
| TianQin | 2035 | Geocentric: 3 (equilateral triangle) | $1.7 \times 10^5$ km | Michelson-type, 1064 nm, 4 W | 0.1 mHz–1 Hz | ILRI 1064 nm | Change in distance: pm |

2021), which share similar objectives in the 0.1 mHz-1 Hz frequency range. These missions are discussed in Zhang et al. (2022).

### 3.3. Satellite-based navigation

Navigation satellites fly in a constellation to provide Position, Navigation and Timing (PNT) services on the ground and in space. The accuracy of the user position provided by such constellations depends on the accuracies of their orbits and satellite clocks (Henkel, 2020). The former is done by precise ground tracking or ranging measurements on-board the satellite (ISL) or both. Besides, the signal timing information is used to synchronize the satellite clocks with stable ground-based clocks. The use of ISLs can improve the Precise Orbit Determination (POD) of such satellites, leading to high-precision positioning (Davis and Gunter, 2022; Li et al., 2019). Moreover, an ISL can be used for data and time transfer among the satellites in the constellation. This section describes the currently operational GNSS and Regional Navigation Satellite System (RNSS) satellites, upcoming CubeSat constellations, and the future lunar navigation service.

#### 3.3.1. GNSS

Global Navigation Satellite Systems (GNSS) denote the worldwide satellite constellations that provide global PNT services. As of now, there are four such systems: American Global Positioning System (GPS), Russian Globalnaya Navigatsionnaya Sputnikovaya Sistema (GLONASS), European Galileo, and the Chinese BeiDou Satellite Navigation System (BDS). All these satellites are spread in MEO, Geostationary Orbit (GEO), and Inclined Geosynchronous Orbits (IGSOs).

The inter-satellite distance of these constellations is determined by ground-based tracking using radio-based ranging and SLR. However, the next-generation GNSS satellites will have crosslinks to perform on-board inter-satellite ranging. The BDS-3 satellites have Ka-band dual one-way pseudo-code ranging systems with centimeter-order precision (Huyan et al., 2020; Xie et al., 2020). The inclusion of these ISL measurements to the POD process reduced the position error by 8 cm and 70 cm for IGSO and GEO satellites, respectively, as compared to POD done only with L-band ground tracking (Lv et al., 2020).

The next generation GLONASS-M/K satellites carry both radio and optical payloads for ISL. The latter is called the Inter-Satellite Laser Navigation and Communication System (ISLNCS) and can measure the distance between two satellites with a precision of 3 cm (Teunissen and Montenbruck, 2017).

The future Galileo Second Generation (G2G) satellites are proposed to be equipped with Optical Two-Way Links (OTWLs) not only with the ground station but also Laser Inter-Satellite Link (LISL). Simulation-based analysis shows that the LISL in combination with OTWL can improve the POD when fewer ground stations are available (Marz et al., 2021). This difference is because OTWL highly depends on the ground station availability and weather conditions, as laser links are sensitive to atmospheric disturbances and a link cannot be established while the sky is covered in clouds.

Another navigation system called Kepler was proposed by the German Aerospace Center. It proposes using laser transceivers for high-speed communication and sub-mm order ranging (Giorgi et al., 2019). The Kepler infrastructure proposes a streamlined approach with minimal ground stations, relying on continuous links with LEO satellites, fixed coordinates, and independent determination of Earth Rotation Parameters for reliable navigation.

Besides the global coverage provided by GNSS, the RNSS constellations improve the dilution-of-precision (DOP) over their respective regions, which is influenced by the satellites' distribution with respect to the user. If the satellites are equally distributed, the DOP will be low, and the position will be precise. There are two regional systems, the Indian Navigation with Indian Constellation (NAVIC) and the Japanese Quasi-Zenith Satellite System

(QZSS). The former provides position accuracy of at least 20 m over the Indian region, and the latter, QZSS, operates at the same frequency as GPS but provides short interval (15 min) orbit and clock updates resulting in m-order accuracy. Although the ISLs are not yet employed for RNSS constellations, they are under consideration for the future QZSS satellites.

### 3.3.2. LEO-PNT

Low Earth Orbit-Positioning, Navigation and Timing (LEO-PNT) is an upcoming European mega-constellation at an altitude of less than 2000 km (Singh et al., 2022). This constellation aims to provide PNT services in regions where GNSS signals are weak or unreliable, like near dense foliage or urban canyons. Due to its proximity to Earth compared to GNSS, the signals received from LEO-PNT will have much higher power. Secondly, it will provide continuous coverage (even on the poles) as the velocities of LEO satellites are much larger than that of MEO satellites. Moreover, the use of CubeSats will also reduce the system complexity. Therefore, LEO-PNT will complement the GNSS constellation to improve the positioning services on the ground. The satellites will perform two-way inter-satellite ranging in the Ka and L-band. Analysis shows that a LEO constellation of 60 satellites with an inter-satellite ranging accuracy of 10 cm and 40 cm can result in a 3D POD accuracy of 2.2 cm and 35 cm, respectively (Li et al., 2019).

### 3.3.3. LCNS

Lunar Communication and Navigation Service (LCNS) is a constellation of four satellites that will be launched in an Elliptical Lunar Fixed Orbit (ELFO) in 2025 as part of ESA 's Moonlight initiative (Melman et al., 2022). It will serve as a navigation and communication gateway in lunar orbit on the road to Mars. All satellites will carry deep-space transponders with ISLs operating at X-band for communication. The same links will also be used for asynchronous ranging and high-precision time transfer. In addition, the satellites will be tracked by SLR stations using retroreflectors.

### 3.3.4. Summary

Satellite constellations providing PNT services for the Earth and the Moon region, given in Table 3, were discussed in this section. The former constellations depended only on ground-based methods for satellite tracking. However, this prevents real-time orbit and clock updates, limiting the PNT accuracy achieved by the user. Therefore, ISLs are also used in the latest navigation satellites for communication, ranging, and time synchronization. The introduction of ISLs can reduce the dissemination latency at the user end from 100 minutes to 5 minutes and increase the POD accuracy from 65 cm to 10 cm (D'Angelo et al., 2012). The overall PNT performance is influenced by the number of satellites in the constellation, the precision of inter-satellite ranging, and the geometric distribution of satellites. A denser constellation with higher ranging precision leads to improved PNT accuracy for users. Additionally, users in closer proximity to the constellation typically experience better PNT performance compared to those farther away. Therefore, to further improve the ranging precision, lasers are being considered for future ISL links (Giorgi et al., 2019).

Table 3
An overview of the present and future navigation constellations with inter-satellite measurements (Teunissen and Montenbruck, 2017; Zhu et al., 2022). CC stands for Control Center, and MS stands for Monitoring Stations.

| | Mission | Year | Orbit/ Configuration | Ground Stations | Inter-satellite measurements | Measurement error | Integration time |
|---|---|---|---|---|---|---|---|
| GNSS | GPS | 1978 | MEO: 24 on 6 orbital planes | CC: 1 (US), | GPS-II/IIIA: IRTR UHF-band, | 0.3 m | – |
| | | | | MS: 16 (Global) | GPS-IIIB: IRTR V-band | proposed | – |
| | GLONASS | 1982 | MEO: Walker 24/3/1 | CC: 1 (Russia), | GLONASS-M/K: IRTR S-band, | 0.4 m | 5 min |
| | | | | MS: 18 (Russia) | GLONASS-K2: ILTR | 0.03 m | – |
| | BeiDou | 2000 | MEO: Walker 27/3/1, | CC: 1 (China), | BDS-3: IRTR Ka-band | <0.1 m | 1.5 s |
| | Galileo | 2011 | MEO: Walker 24/3/1 | CC: 2 (EU), MS: >20 (Global) | G2G: ILTR | 0.01 m | 100 s |
| | | proposed | LEO: Walker 6/2/1 | CC: 1 | Kepler: ILTR | sub–mm | – |
| RNSS | QZSS | 2010 | GEO: 1, IGSO: 3 | CC: 1 (Japan), MS: 16 (Japan) | – | – | – |
| | NavIC | 2018 | GEO: 3, IGSO: 4 | CC: 1 (India), MS: 16 (India) | – | – | – |
| Others | LCNS | 2025 | ELFO: 4 | – | IRTR X-band + time transfer | – | – |
| | LEO-PNT | proposed | LEO: ~12 | – | IRTR Ka/L-band | few dm | – |

### 3.4. Earth observation

Earth Observation (EO) satellites are orbiting around the Earth for monitoring and collecting data continuously. They capture high-resolution images, measure environmental parameters, and track changes on the Earth's surface, atmosphere, and oceans. The data obtained is crucial for environmental monitoring, climate studies, disaster management, agriculture, etc. (Zhao et al., 2022). To enhance temporal resolution and capture the dynamic nature of Earth's processes, multiple satellites are often employed in coordinated formations. The space missions with multiple satellites whose data resolution depends upon the accuracy of active inter-satellite distance measurements are discussed in this section.

#### 3.4.1. Tandem-X/ TerraSAR-X

Synthetic Aperture Radar (SAR) works by transmitting microwave pulses toward the Earth's surface and recording the signals reflected back. The radar antenna is mounted on the satellite, and as the platform moves, a synthetic aperture is created by combining the radar returns over a series of positions. This synthetic aperture allows SAR to achieve high spatial resolution. SAR can be used in interferometric mode (Interferometric Synthetic Aperture Radar (InSAR)) to measure ground deformations with high precision. By comparing phase differences between two or more SAR images acquired at different times or from different angles, InSAR can detect surface movements. Many satellite formations are working on this principle to study small changes in the terrain, such as monitoring movement in ice and tectonic shifts.

Launched in 2010, TanDEM-X: TerraSAR-X Add-oN for Digital Elevation Measurement (TDX) is a German radar satellite that flies in a close formation with its twin TerraSAR-X (TSX) (Zink et al., 2006). Both satellites carry SAR sensors operating in the X-band (3 cm wavelength) to generate digital elevation models of Earth with 2 m vertical accuracy. The distance between the satellites, also called the baseline, varies from 120 m to several km and must be determined with a 1 mm 1D accuracy (Jäggi et al., 2012). The Tracking, Occultation and Ranging (TOR) payload on each satellite is responsible for these measurements. It consists of a dual-frequency Integrated GPS and Occultation Receiver (IGOR) to perform differential carrier phase measurements. Post-processing of the mission data shows a baseline performance close to the mission requirements, but independent SAR calibration data is required to achieve the 1 mm target (Jäggi et al., 2012). The Spanish satellite called PAZ also joined the formation in 2018.

Tandem-L is a follow-up mission proposal based on the same concept, except that it performs SAR in the L-band (23.6 cm wavelength). The purpose of the mission is to measure forest biomass and its temporal variation using a pair of satellites at an altitude of 745 km separated by 1–18 km (Moreira et al., 2015).

#### 3.4.2. CHESS

The Constellation of High Energy Swiss Satellites (CHESS) program consists of two missions, CHESS-Pathfinder and CHESS-Live (Fausch et al., 2022). The former will be launched in 2026 and will provide near real-time data of Earth's upper atmosphere using two nanosatellites. One satellite will be in a circular Sun-Synchronous Orbit (SSO) at 550 km to study the impact of the Sun on the exosphere. Another will be in an elliptical orbit at 400 km × 1000 km to establish altitude profiles and study temporal effects. Each satellite carries a mass spectrometer for chemical composition analysis and GNSS receivers for POD and drag computation. Currently, there is no ISL between the satellites. However, to estimate drag every 30 minutes, cm to dm-level position knowledge is required. The findings from CHESS-Pathfinder will be used to determine the parameters of the follow-up mission, CHESS-Live, consisting of more than eight satellites.

#### 3.4.3. Summary

This section covers two distinct Earth Observation missions, as given in Table 4. The Tandem-X/L mission generates Earth's digital elevation models through the use of InSAR, while the CHESS mission is a future constellation to analyze the composition of the upper atmosphere. Due to operations near Earth, both missions employ dual-frequency GNSS receivers and retroreflectors for POD. GNSS can provide mm-level position accuracy for LEO satellites. For missions with more stringent requirements or those requiring data/time transfer, alternative tracking methods, such as those used in the GRACE missions (Section 3.1), can be employed.

### 3.5. Constellation control

A satellite constellation is a group of satellites working collectively toward a common objective: they operate inde-

Table 4
An overview of missions using inter-satellite tracking for Earth Observation.

| Mission | Year | Orbit/ Configuration | Inter-satellite distance | Inter-satellite measurements | Measurement error | Integration time |
|---|---|---|---|---|---|---|
| Tandem-X/ TerraSAR-X | 2010–2026 | LEO: 2, Helical Tandem | 120 m– few km | GNSS L-band | 1 mm | 10 s |
| Tandem-L | 2024–2036 | LEO: 2, Helical Tandem | 1–18 km | GNSS L-band | 1 mm | – |
| CHESS-Pathfinder | 2026 | SSO: 1, Elliptical: 1 | 100–1500 km | GNSS L-band | cm-level | – |
| CHESS-Live | – | SSO, Elliptical: >8 | – | GNSS L-band | cm-level | – |

pendently, taking measurements from multiple angles and perspectives. This enables the study of spatial and temporal changes in physical events. Because of their independence, these satellites do not require precise knowledge of their neighboring satellites. However, maintaining and controlling the constellation does require precise knowledge of each satellite's position. Therefore, having accurate information about inter-satellite distances can significantly improve the POD of such constellations. This section will discuss three missions, namely Swarm, CYGNSS, and Q4 within this context. It is crucial to note that the classification is based on the utilization of inter-satellite measurements and not on the missions' application.

#### 3.5.1. Swarm

The Swarm satellite constellation was launched in 2014 to create a highly detailed survey of Earth's geomagnetic field and its temporal evolution. Initially, it consisted of three satellites, of which two (Swarm-A/C) are in the same polar orbit, and one is in a higher polar orbit (Swarm-B) (Friis-Christensen et al., 2006). The distance between the Swarm-A and Swarm-C satellites varies from 30–180 km, and between Swarm-A/C and Swarm-B from 50–3500 km (Mao et al., 2019).

The Swarm satellites function independently of one another and do not have any ISL because the mission objectives do not directly depend upon precise inter-satellite distance measurements. Nevertheless, precise position knowledge, obtained using the on-board GPS receivers, is still needed to achieve scientific objectives and avoid collisions. In addition, the Laser Retro-Reflectors (LRRs) present on-board the satellites are used to validate the orbits using SLR data. Validation studies have demonstrated a model-limited accuracy of 1–2 cm in the reduced-dynamic precise science orbits (van den Ijssel et al., 2015; Montenbruck et al., 2018).

#### 3.5.2. CYGNSS

The Cyclone Global Navigation Satellite Systems (CYGNSS) was launched in 2016 to study the formation and evolution of tropical cyclones (Ruf et al., 2012). It is a constellation of eight micro-satellites in LEO, orbiting in pairs with a separation of 12 minutes between them. Each satellite carries the Delay Dapper Mapping Instrument (DDMI), which receives the GPS signals reflected off the ocean, providing information on the surface-level wind speed. The collected data is directly downlinked to the ground stations, and no ISL is needed. However, the constellation needs to be controlled to account for variations in trajectory caused by orbital perturbations. Therefore, GPS receivers are installed on each satellite to keep track of its position with meter-order accuracy, and the orbit is maintained using differential drag.

In addition, data collected by the CYGNSS mission has also been exploited to perform ocean altimetry; however, the meter-order orbit accuracy was found to be a limiting factor in achieving altimetry accuracy (Li et al., 2020). Although post-processing techniques can lower these to centimeter-level (Conrad et al., 2023), ISLs can be more useful as they eliminate the need for extensive post-processing.

#### 3.5.3. Q4

Q4 is a mission concept proposed by NASA for the technology demonstration of the novel Inter-Satellite Optical Communicator (ISOC). The mission will consist of a swarm of four 6U-CubeSats in the LEO, each equipped with it and, using an array of 1 W 850 nm laser-diode telescope and photodetectors, the terminal will be able to provide 1 Gbps data rate (using NRZ OOK modulation) at distances up to 200 km (Velazco and Vega, 2020). In addition, ISOC consists of an Angle-of-Arrival (AoA) system, which will continuously measure the azimuth and elevation of the transmitting satellite using pulses. The inter-satellite distance can be computed by post-processing these pulses for TOF measurements (Velazco et al., 2020). Besides Q4, ISOC is also under consideration as a payload for two large swarm missions, CubeSat Array for the Detection of RF Emissions from Exoplanets (CADRE) (De Kok et al., 2020) and INterplanetary SPace InteRnEt (INSPIRE) (Velazco, 2023b).

Another version of the ISOC is developed concurrently to serve the communication and navigation needs for future cislunar missions. This terminal, called Omindirectional Optical Terminal (OOT), will consist of six telescopes operating at the wavelength of 1550 nm. It is equipped with six fast photodetectors for high data rates and twenty external PIN photodetectors for AoA measurements (Velazco, 2023a). The OOT will be able to provide 10–100 Gbps over distances spanning from a few kilometers to a few thousand kilometers. The OOT transmits a single laser beam composed of two types of pulses: very short-width pulses for communication and wider pulses for AoA, allowing an accuracy of millidegrees for AoA measurements.

#### 3.5.4. Summary

In the missions described above, GNSS receivers are the dominant technology to obtain absolute satellite positions with meter-level accuracy. This accuracy level is refined to centimeter-level when coupled with SLR data. However, new concepts of omnidirectional laser terminals are being studied to enable accurate AoA and TOF measurements for inter-satellite distance computation. Table 5 outlines the key specifications for the missions under consideration. It is noteworthy that the constellations with shorter inter-satellite distances necessitate more precise position knowledge as compared to those with longer distances.

Table 5
An overview of space missions using inter-satellite tracking for constellation control.

| Mission | Year | Orbit/ Configuration | Inter-satellite distance | Inter-satellite measurements | Measurement error |
|---|---|---|---|---|---|
| Swarm | 2014 | LEO Polar: 3 | 30–3500 km | GNSS L-band | 1–2 cm |
| CYGNSS | 2016 | LEO: 8 (4 pairs) | 5400 km | GNSS L-band | m-level |
| Q4 | concept | LEO: 4 | 200 km | ILTR 850 nm (AoA) | – |
| Future CisLunar | concept | Moon | 1–1000 km | ILTR 1550 nm (AoA) | AoA: millidegree |

### 3.6. Space exploration

Space exploration expands our understanding of the universe. Inter-satellite tracking can be invaluable for satellites, particularly when GNSS signals become increasingly faint at greater distances from Earth. This section will delve into the applications of inter-satellite tracking, spanning heliophysics, astrophysics, and planetary exploration. Seven missions are discussed, namely, MMS, HelioSwarm, ETP, HERMES-TP/SP, CAMELOT, Trilogy, and low-frequency interferometry.

#### 3.6.1. MMS

The Magnetospheric Multiscale Mission (MMS) has been studying the Earth's magnetosphere since 2015 using a tetrahedral formation of four spacecraft. It explored the magnetic interaction on the Sun-facing side of the Earth in the first phase and night side at a later stage. The relative spacing varied between 10 and 160 km in the former and 30 to 400 km in the latter phase (Burch et al., 2016). All spacecraft carry the inter-satellite ranging system developed by NASA Goddard Space Flight Center (GSFC). It consists of a GPS receiver, *Navigator*, which is capable of detecting weak signals, and the flight software Goddard Enhanced Onboard Navigation System (GEONS) for onboard orbit determination (Winternitz et al., 2017a; Winternitz et al., 2017b). In-orbit data has demonstrated that the inter-satellite ranging system can achieve range measurements with the required accuracy of 1% of the separation distance, translating to maximum accuracy between 100 m and 4 km (Farahmand et al., 2017). Although MMS currently only relies on the data from the GPS receiver, a 0.25 W S-band crosslink transceiver was proposed in the initial mission design phase to perform communication and one-way ranging. However, during the TRL-6 mission study phase, it was found that critical science objectives could be fulfilled without the crosslink. Hence, the science was descoped, and the transceiver was removed from the inter-satellite ranging system (Long et al., 2015; Bamford et al., 2009). The MMS mission demonstrated that if GPS receivers can detect transmissions from L-band sidelobes, they can be used for navigation as far as in the lunar orbit (Winternitz et al., 2017b).

#### 3.6.2. HelioSwarm

HelioSwarm is planned for launch in 2028 to observe the solar wind and understand the plasma turbulence processes (Plice et al., 2019). Unlike previous missions, like MMS, which probe only a single scale at a time, HelioSwarm will provide multi-scale measurements simultaneously. Using a swarm of nine satellites in a lunar orbit, it will take measurements along 36 baselines of varying lengths (50–3000 km). Of these nine spacecraft, one large spacecraft will act as the hub, and eight smaller ones will act as nodes. The hub will have S-band links with all nodes and the DSN. The crosslinks with each node will be used to perform two-way inter-satellite ranging, and measurements will be taken every 5 s for 30 minutes daily for one node at a time. Ranging will not be conducted when data transfer with the nodes or DSN is in progress (Policastri and Woodburn, 2019). The inter-satellite separation should be known with an accuracy of 10% of the distance to resolve the propagation directions of solar waves, i.e., 5–300 km (Klein et al., 2023).

#### 3.6.3. Gamma-ray burst detection

A Gamma-Ray Burst (GRB) is a highly energetic and intense burst of gamma rays that can release a large amount of energy in a very short period. The detection of such events is of high interest for advancing our understanding of the universe's history, extreme astrophysical phenomena, and fundamental physics. The INTErnational Gamma-Ray Astrophysics Laboratory (INTEGRAL) (Savchenko et al., 2017) and Fermi (Goldstein et al., 2017) missions have been spotting these bursts for more than two decades. However, the appearance of GRBs for a fraction of a second makes it challenging to locate their origins using a single spacecraft. Therefore, the latest studies on GRB detection are analyzing the use of CubeSat constellations, not only to cover the entire sky but also to measure the difference in detection time on different CubeSats as this will aid in triangulating the origin of a GRB. Hence, the main requirement of such missions is accurate positioning and absolute and relative timing of the satellites in the constellations.

Many astrophysics missions can be found in literature (Bloser et al., 2023): the High Energy Rapid Modular Ensemble of Satellites - Technologic and Scientific Pathfinder (HERMES-TP/SP) and Cubesats Applied for MEasuring and LOcalising Transients (CAMELOT) are future CubeSat constellations being developed for GRB detection and planned for launch in 2024. HERMES-TP/SP requires absolute timing accuracy in the order of hundreds of ns (Fiore et al., 2020; Sanna et al., 2020; Evangelista et al., 2020), whereas, for the CAMELOT mission, the requirement is hundreds of μs (Werner et al., 2018). GPS receivers

will be used on both missions to synchronize on-board clocks and time-tag transient events. The CAMELOT satellites will also have ISLs for communication.

#### 3.6.4. Low frequency interferometry

Since the ionosphere absorbs low-frequency electromagnetic waves (~10–15 MHz), radio observations at these wavelengths can only be done from space. Radio interferometry is a technique that allows the use of multiple smaller antennas instead of a larger one, enabling high-resolution sky imaging in the lower frequency range and helping to understand the evolution of solar transients like Coronal Mass Ejections (CMEs). Many missions have been proposed in the past to launch a space-based radio interferometer using 12–16 CubeSats, like Astronomical Low Frequency Array (ALFA) (Jones et al., 2000), Solar Imaging Radio Array (SIRA) (MacDowall et al., 2005), and, Solar Observing Low-frequency Array for Radio Astronomy/ Separated Antennas Reconfigurable Array (SOLARA/SARA) (Knapp et al., 2013); however, they could not fly due to high cost and complexity. Nevertheless, if such a mission would be considered in the future, real-time baseline measurements should have an accuracy of at least $0.1\lambda$ (2–3 m) to allow a good correlation of the signals received at different spacecraft (Oberoi and Pinçon, 2005).

In addition, a mission concept called Orbiting Low Frequency Array for Radio Astronomy (OLFAR) is currently under study: it aims to detect the signals in the frequency range 0.1–30 MHz using a swarm of 10–50 nanosatellites with a baseline of 100 km in the lunar orbit (Dekens et al., 2013). All satellites will have ISL at both high and low frequencies, the former for communication and the latter for timing synchronization and ranging (Karunanithi et al., 2019).

#### 3.6.5. Trilogy

Trilogy is a conceptual mission that aims to measure the change in the solar system scale (distance between planets), perform tests of relativity, and improve ephemerides (Smith et al., 2018). It is believed that the conversion of hydrogen to helium within the Sun's interior leads to a slight decrease in its mass and, consequently, a change in the orbits of planets. Hence, Trilogy will use the formation of three spacecraft in orbits around Mars, Venus, and Earth and study the change in inter-satellite distances over several years. The trajectory of the planet's center of mass will be derived from the resulting range and range-rate observations. The distance between each pair of planets varies in the order of a few meters over 1500 days (Smith et al., 2018). Inter-satellite ranging with an accuracy of a few centimeters is required over interplanetary distances ($10^7$ km). Therefore, a transponder-based asynchronous laser ranging system is being considered for this mission.

#### 3.6.6. ETP

Europa Tomography Probe (ETP) was proposed as a piggyback mission on the Europa Clipper (Notaro et al., 2020) to be inserted in a polar orbit around Europa. ETP aimed to characterize the interior structure of the Jovian Moon by measuring the time-varying magnetic field at different frequencies. ETP was also proposed to perform a two-way coherent X-band ISL with the mothercraft for communication and Doppler measurements. The latter would help to determine the static gravity field of Europa with high resolution, improving the accuracy of the Moon's rotational state. Moreover, the Doppler observables would also improve the radial positioning of the mother spacecraft relative to Europa at a level of a few meters (Di Benedetto et al., 2019). The accuracy of Doppler measurements achieved in the simulations was 0.1 mm/s at an integration time of 60 s, comparable to the Ka-band tracking from the ground (Notaro et al., 2020).

#### 3.6.7. Summary

This section outlined a diverse range of space exploration applications. As previously discussed, LEO missions predominantly utilize GNSS receivers to achieve precise positioning and timing data. In contrast, satellites operating in lunar orbits or even farther into deep space employ alternative methodologies, such as radio/laser transponder ranging or Doppler measurements, to compute accurate position information. These missions show the adaptability and innovation needed for space exploration. The missions discussed in this section, along with X-ray Evolving Universe Spectroscopy (XEUS) (Bavdaz et al., 2002; Marcos et al., 2004; ESA, 2004) and InfraRed Astronomy Satellite Swarm Interferometry (IRASSI) (Linz et al., 2020; Buinhas et al., 2018), explained by Zhang et al. (2022), are summarized in Table 6.

### 3.7. Technology demonstration

This category pertains to space missions specifically engineered to demonstrate novel technologies. Therefore, their data products do not depend on inter-satellite distance measurements but rather showcase the capabilities of the utilized technologies. Two such missions, CLICK and CPOD, are discussed.

#### 3.7.1. CLICK

The CubeSat Laser Infrared CrosslinK (CLICK) mission is a technology demonstration for laser crosslinks for satellite swarms. It consists of three 3U CubeSats in LEO. CLICK-A was launched in 2022 and demonstrated a downlink to an optical ground station at 10 Mbps. CLICK-B and CLICK-C are planned for launch in 2024 and will carry a laser transceiver operating at 1550 nm to

Table 6
An overview of satellite constellations requiring inter-satellite tracking for space exploration. The last two missions are explained in Zhang et al. (2022) and are included here for completeness.

| Mission | Year | Orbit/ Configuration | Inter-satellite distance | Inter-satellite measurements | Measurement error |
|---|---|---|---|---|---|
| MMS | 2015 | HEO: 4 (tetrahedral) | 10–160 km 30–400 km | GNSS L-band | 1.5 km |
| HERMES-TP/SP | 2023 | LEO: 6 (equatorial) | few 1000 km | GNSS L-band | Timing: 181 ns |
| HelioSwarm | 2028 | Moon: 9 (1 hub + 8 nodes) | 50–3000 km | IRTR S-band | 5–300 km |
| CAMELOT | – | LEO: 9 (on 3 orbital planes) | few 1000 km | GNSS L-band | Timing: <100 us |
| Low-frequency interferometry | concept | Earth/Moon | – | – | 2–3 m |
| Trilogy | under study | Mars, Venus, Earth: 3 | ~10 Mkm | ILTR 1550 nm | cm-level |
| ETP | cancelled | Europa: 2 | <0.1 Mkm (short-range), 0.1–1 Mkm (long range) | IRDT X-band | mm-level |
| IRASSI | proposed | Sun-Earth L2: 5 | 7–850 m | ILRI | 1 μm |
| XEUS | cancelled | Sun-Earth L2: 2 | 0.12–30 km | ILRR | 0.1 mm |
| | | | 50–120 m | ILRI | 3.5 μm |

perform two-way ISL at 20 Mbps between 25 and 580 km. In addition, the satellites will also measure the travel time of laser pulses using a Chip-Scale Atomic Clock (CSAC) to perform precision ranging with accuracy better than 50 cm (Tomio et al., 2022; Serra et al., 2021; Cahoy et al., 2018).

### 3.7.2. CPOD

The CubeSat Proximity Operations Demonstration (CPOD) mission was launched in May 2022 to demonstrate the Rendezvous, Proximity Operations and Docking (RPOD) of two 3U CubeSats in LEO. However, the mission ended in June 2023 due to the depletion of spacecraft propellant due to multiple rendezvous attempts. The satellites navigated relative to each other and then performed proximity operations to reach a specific relative range, and then docking would have taken place. An ISL utilizing a 2.4 GHz transceiver was used to provide data and range information up to several kilometers range (Bowen et al., 2015). Although the CPOD mission could not be completed, the robustness and viability of the RPOD algorithm and strategy were confirmed.

### 3.7.3. Summary

This section gives an overview of the missions designed to demonstrate new technologies for formation control. Table 7 gives the specifications of the reviewed missions, CLICK and CPOD. Additionally, the missions discussed by Zhang et al. (2022) falling into this category, such as Gemini (Gill et al., 2001), PRecursore IperSpettrale della Missione Applicativa (PRISMA) (Persson et al., 2006; Persson et al., 2005; Gill et al., 2007), Canadian Advanced Nanospace eXperiment 4 & 5 (CanX-4/5) (Eyer et al., 2007), and Proba-3 (Llorente et al., 2013; Wishart et al., 2007), are also included in the table.

## 4. Discussion

This section provides a detailed discussion of the investigated missions that employ inter-satellite tracking. Initially, the discussion delves into the mission categories, the tracking methods utilized, and the precision requirements for different applications. Subsequently, this analysis serves as the basis for identifying potential applications for tracking using LCTs.

### 4.1. Missions requirement analysis

The 44 missions studied were systematically classified into seven distinct application areas based on their utilization of tracking measurements. The survey unveiled the use of six distinct methods for inter-satellite tracking: GNSS, Inter-satellite Radio Transponder Ranging, Inter-satellite Laser Transponder Ranging, Inter-satellite Laser Retroreflector Ranging, Inter-satellite Laser Ranging Interferometry, and Inter-satellite Radio Doppler Tracking (refer

Table 7
Space missions designed for technology demonstration of inter-satellite tracking methods. The last four missions are explained in Zhang et al. (2022) and are included here for completeness.

| Mission | Year | Orbit/ Configuration | Inter-satellite distance | Inter-satellite measurements | Measurement error |
|---|---|---|---|---|---|
| CLICK | 2022 | LEO: 3 | 25–580 km | ILTR 1550 nm | 50 cm |
| CPOD | 2022–2023 | LEO: 2 | 0.5 m–25 km | IRTR UHF-band | – |
| Gemini | 2001 | LEO: 2 | 1–250 km | GNSS | cm–m |
| | | | <1 km | ILRI | 10 μm |
| PRISMA | 2010 | LEO: 2 | 250 m–10 km | IRTR S-band, GNSS | 1–10 cm |
| CanX-4/CanX-5 | 2014 | LEO: 2 | 50–1000 m | IRTR S-band, GNSS | 10 cm |
| Proba-3 | 2023 | HEO: 2 | 25–250 m | IRTR (SDR-based) | 25 cm |

to Section 2 for detailed descriptions). Additionally, many missions employed a combination of these methods to achieve their desired inter-satellite tracking requirements.

Figure 3 depicts the distribution of missions and their corresponding number of satellites across the seven application areas that require inter-satellite tracking. While missions within the same category share common objectives, the number of satellites deployed can significantly differ based on mission-specific requirements and goals. For instance, missions designed to provide global positioning and navigation services typically necessitate a large number of satellites. Meanwhile, Earth observation and satellite gravimetry missions commonly use pairs of satellites in close formations to capture minor and local variations near Earth and other celestial bodies. However, emerging concepts such as MAGIC (Section 3.1.3) and CHESS-Live (Section 3.4.2) propose the use of satellite constellations, enabling simultaneous measurements from multiple perspectives, potentially reducing post-processing times. The analysis reveals that gravimetry, navigation, and space exploration are the primary applications requiring inter-satellite tracking measurements in past and upcoming missions. Furthermore, satellite gravimetry and gravitational wave detection missions measure minute variations in satellites' orbits and hence rely significantly on inter-satellite tracking to achieve their objectives. For most missions across other categories, while an ISL enhances the scientific or commercial return, they can still operate effectively without it. Technology demonstration missions were excluded from further analysis as their primary focus is testing and validating new space technologies.

Figure 4 explores the relationship between the mission orbital regimes and the employed tracking methods. It showcases the versatility of inter-satellite tracking measurements, applicable from the low-earth orbit to deep-space. Satellites in distant orbits, often used for scientific missions, such as gravitational wave detection, gravimetry, and space exploration, operate at vast inter-satellite distances on the order of millions of kilometers. Given the significant variation in signal frequency over such distances, IRDT or ILRI measurements are commonly employed. IRTR measurements are employed for missions up to the Lunar orbit, while ILTR is being considered even for deep-space applications. Conversely, GNSS is the most common method employed for applications near the Earth orbit, particularly for Earth Observation, as also evident from Fig. 5.

Figures 5 and 6 illustrate the precision demands for different applications and the achievable precision of various tracking methods, respectively. Missions for gravitational wave detection and satellite gravimetry require exceptionally high range-rate precision (pm/s to μ/s) and thereby rely on ILRI measurements. In contrast, applications with less stringent requirements (error more than cm-level) leverage GNSS for orbit maintenance. However, some GNSS recei-

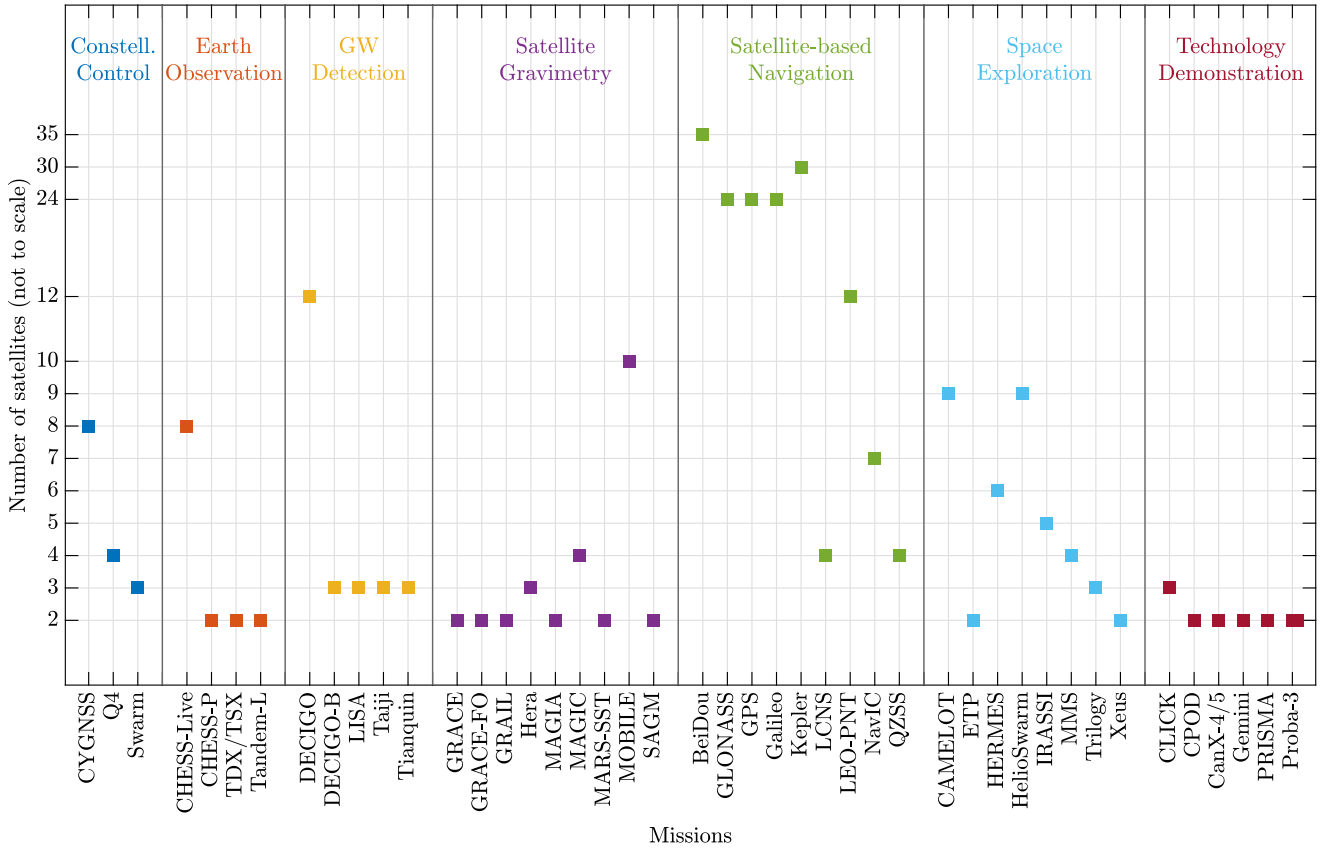


Fig. 3. Missions versus the number of satellites, separated into seven application categories depicted by vertical sections.

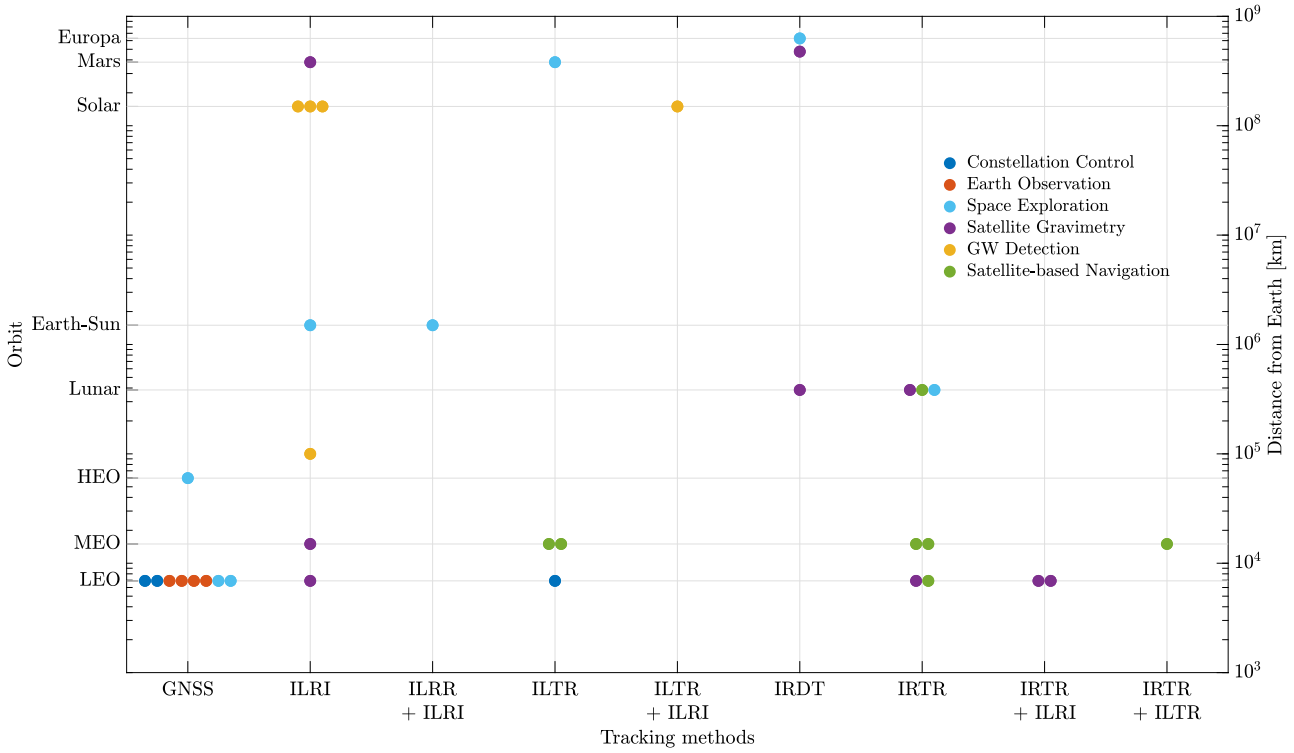


Fig. 4. Orbits of interest from the discussed space missions versus the tracking methods employed. The colors represent the category of application. (For interpretation of the references to colour in this figure legend, the reader is referred to the web version of this article.)

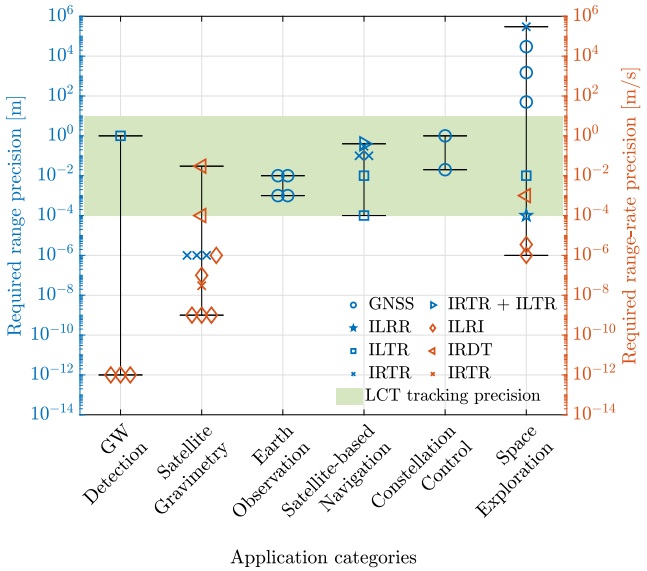


Fig. 5. A graph of range (blue) and range-rate (orange) measurement precision versus the applications. The markers represent the tracking methods employed for these measurements. The shaded region represents the expected ranging precision of LCTs. (For interpretation of the references to colour in this figure legend, the reader is referred to the web version of this article.)

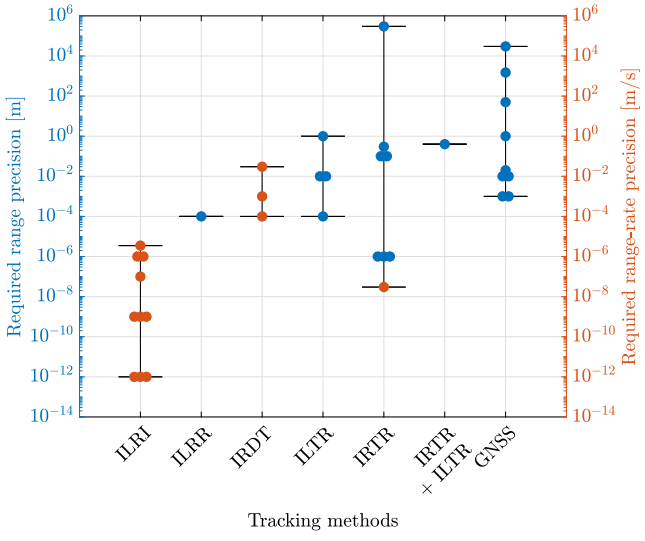


Fig. 6. A graph of range (blue) and range-rate (orange) measurement precision versus tracking methods. (For interpretation of the references to colour in this figure legend, the reader is referred to the web version of this article.)

vers (as on TerraSAR-X) can provide mm-level accuracy for satellites near Earth, making it suitable for Earth Observation missions. To provide better PNT services to the users, future navigation constellations are proposing the use of ILTR in addition to existing IRTR for more accurate inter-satellite tracking.

A notable trend is the prevalent use of IRTR for direct range measurements, fulfilling up to sub-micrometer tracking needs. However, a significant limitation of this approach is that the ranging signal is multiplexed with

the communication one. It distributes the available onboard power between ranging and communication functions, leading to a substantial reduction in the range resolution as well as the data rate. For example, the Mars Reconnaissance Orbiter (MRO) is capable of a maximum data rate of 0.48 Mbps during ranging operations, significantly lower than the 5.2 Mbps achievable under normal operational circumstances (Hamkins et al., 2015). *Hence, ongoing research is dedicated to eliminating the need for a separate ranging signal and utilizing communication signals for ranging purposes* (Andrews et al., 2010; Hamkins et al., 2015; Hamkins et al., 2016a; Hamkins et al., 2016b; Vilnrotter and Hamkins, 2019; Turan et al., 2023).

Nevertheless, a noticeable shift is underway, with upcoming missions showing an increasing preference for transponder-based laser ranging methods (ILTR). This shift aligns with the broader trend in space communication, which is progressively transitioning from radio to optical frequencies. Furthermore, the field of laser transponder ranging is relatively new, with the current research actively exploring data-aided laser ranging (Net and Hamkins, 2020; Net, 2023). The integrated communication and ranging system being developed for the Kepler navigation constellation is one such example offering sub-mm range precision (Giorgi et al., 2019). However, it does not perform communication and ranging functions at the same time. Additionally, the CLICK satellites (Section 3.7.1) recently demonstrated inter-satellite ranging with 50 cm accuracy using a 20 Mbps optical data link (Grenfell, 2024), however, communication and ranging were not done at the same time. The shaded region in Fig. 5 shows the potential tracking precision achievable with LCTs. This transition to ILTR highlights the growing potential for improved range measurements in future space missions.

### 4.2. Potential applications of laser communication terminals for tracking

Based on the above analysis of precision requirements for different applications and the capability of LCTs to achieve sub-millimeter ranging precision, the potential applications of LCTs for tracking are discussed here. The question of how and whether LCTs can achieve this level of precision remains open, but it is a prospect suggested by the current literature.

The shaded region in Fig. 5 illustrates that the expected tracking precision of LCTs in most applications is comparable to or better than existing tracking methods, except for ILRI. This indicates that future satellites equipped with LCTs for communication could eliminate the need for separate, dedicated tracking instruments in a wide range of applications, except gravitational wave detection and satellite gravimetry of Earth and Moon. Since the gravity models of the Earth and Moon are well refined due to data provided by GRACE and GRAIL missions, further improvements will require measurements accurate than sub-micrometer level beyond the capability of present LCTs, may be achievable in the future. Besides, these missions do not require large amounts of data transfer, making them not suited for combined communication and ranging systems. Therefore, dedicated ILRI systems remain the preferred choice for these specific applications. Additionally, the feasibility of replacing range-rate measurements with range measurements from LCTs will depend on the nature of the signal being measured; if the quantity changes rapidly, range-rate may be more effective than range.

For gravimetry beyond the Moon and deep-space exploration, LCT tracking could provide a better alternative to the currently employed IRDT measurements. In space exploration missions near Earth, while GNSS can fulfill the position requirements, direct range measurements using ILTR or IRTR can enable additional scientific investigations. For example, in the case of the MMS mission (Section 3.6.1), the inability to incorporate a transceiver for communication and ranging resulted in the descoping of original science objectives. Consequently, the mission was limited to achieving objectives that could be accomplished solely with GNSS capabilities. If LCT were employed, this limitation would have been mitigated.

The integration of ILTR with existing methods could enhance tracking precision in satellite-based navigation, as proposed by future GLONASS and Kepler satellites. Additionally, accurate relative positioning is also crucial for satellite constellations to ensure collision avoidance and facilitate scientific observations. For instance, the CYGNSS mission (Section 3.5.2) performed ocean altimetry but was limited by the meter-level orbit accuracy from GNSS. However, the feasibility of LCT to replace GNSS for altimetry will depend on the link geometry. In such cases, ILTR or IRTR measurements can substantially improve the orbit accuracy, enabling more precise scientific observations and mission objectives. While mega-constellations like Starlink, Kuiper, and Lightspeed also require tracking for constellation control, their needs are currently met by ground-based tracking methods. As such, they fall outside the scope of this paper, which focuses on missions using inter-satellite tracking. Nevertheless, recent studies have demonstrated the capability of inter-satellite tracking for these constellations, highlighting its potential benefits for localization and collision avoidance (Spring-Turner and Thilak Rajan, 2022; Chaudhry and Yanikomeroglu, 2021). Moreover, since they already use lasers for communication, they are also a potential application for LCT-based tracking.

In summary, tracking using LCTs presents a promising prospect for a wide range of space applications. The actual capability of LCT to replace existing methods will depend upon the link geometry and mission objectives. However, a key challenge lies in developing a system that can perform ranging using existing state-of-the-art LCTs without compromising their data rates. Further research on determining and modeling systematic errors within LCTs is imperative to establish achievable performance levels. This research will be instrumental in realizing the full potential

of ILTR for future space missions, paving the way for groundbreaking scientific discoveries and advancements in space exploration.

## 5. Conclusions

This study explored the diverse applications of inter-satellite tracking in space missions by analyzing 44 missions. This expanded the scope of the previous work by Zhang et al. (2022) by not only including 33 additional missions but also by categorizing them into seven distinct application areas based on their need for tracking measurements. This categorization provides valuable insights into the specific tracking needs of different applications. The analysis focused on the employed tracking methods and their corresponding precision in each application. The key domains where inter-satellite measurements are paramount include satellite gravimetry, satellite-based navigation, and gravitational wave detection. These areas exhibit varying precision requirements, with gravitational wave detection missions demanding the highest and space exploration missions requiring the lowest.

For missions operating near Earth, GNSS is a suitable choice, providing sufficient accuracy. In contrast, for missions farther away, Inter-satellite Radio Transponder Ranging (IRTR) has historically been favored, delivering precision in the range of centimeters to meters. However, an emerging trend is the increasing adoption of Inter-satellite Laser Transponder Ranging (ILTR), offering sub-millimeter precision. It can benefit applications requiring inter-satellite tracking for satellite gravimetry beyond the Moon, satellite-based navigation, constellation control, and deep-space exploration.

The integration of ranging capabilities with Laser Communication Terminals presents a promising prospect. However, adapting existing LCTs for ranging purposes while maintaining data rates poses a significant challenge that requires further investigation. In conclusion, this study presents a positive outlook on the future of inter-satellite laser tracking and emphasizes the need for further research to maximize its potential and address challenges.

## Declaration of Competing Interest

The authors declare that they have no known competing financial interests or personal relationships that could have appeared to influence the work reported in this paper.

## Acknowledgments

The authors would like to thank the support from the Dutch Research Council (NWO) for funding the Perspective Project P19-13, ”Optical Wireless Super Highways”. The authors declare that they have no relevant or material financial interests that relate to the research described in this paper.

## References

Amaro-Seoane, P., Audley, H., Babak, S., et al., 2017. Laser Interferometer Space Antenna. arXiv e-prints, (p. arXiv:1702.00786). doi:10.48550/arXiv.1702.00786.

Amazon (December 2023). Amazon’s Project Kuiper completes successful tests of optical mesh network in low Earth orbit. US About Amazon. URL: https://www.aboutamazon.com/news/innovation-at-amazon/amazon-project-kuiper-oisl-space-laser-december-2023-update Accessed: April 5, 2024.

Andrews, K., Hamkins, J., Shambayati, S., et al., 2010. Telemetry based ranging. IEEE Aerospace Conference. https://doi.org/10.1109/AERO.2010.5446926.

Bamford, W., Mitchell, J., Southward, M. et al., 2009. GPS navigation for the magnetospheric multiscale mission. In: 22nd International Technical Meeting of the Satellite Division of the Institute of Navigation (ION GNSS 2009) (pp. 2270–2280). volume 4. URL: https://www.ion.org/publications/abstract.cfm?articleID=8554.

Bavdaz, M., Peacock, A., Laan, T.V.D., et al., 2002. The XEUS: Approaches to mission design. Proceedings of SPIE - The International Society for Optical Engineering volume 4851, 396–404. https://doi.org/10.1117/12.461732.

Bender, P.L., Wiese, D.N., Nerem, R.S., 2008. A possible Dual-GRACE mission with 90 degree and 63 degree inclination orbits. In: Proceedings of the 3rd International Symposium on Formation Flying, Missions and Technologies. European Space Agency Symposium Proceedings, SP-654 jILA Pub (pp. 1665–1669). volume 8161. URL: https://api.semanticscholar.org/CorpusID:123769230.

Bertone, S., Le Poncin-Lafitte, C., Rosenblatt, P., et al., 2018. Impact analysis of the transponder time delay on radio-tracking observables. Adv. Space Res. 61 (1), 89–96. https://doi.org/10.1016/j.asr.2017.09.003.

Bloser, P., Murphy, D., Fiore, F., et al., 2023. CubeSats for Gamma-Ray Astronomy. In: Bambi, C., Santangelo, A. (Eds.), Handbook of X-ray and Gamma-ray Astrophysics. Springer, Singapore, pp. 1–33. https://doi.org/10.1007/978-981-16-4544-0_53-1.

Bocanegra-Bahamőn, T.M., Molera Calvés, G., Gurvits, L.I., et al., 2018. Planetary radio interferometry and doppler experiment (pride) technique: A test case of the mars express phobos flyby. Astron. Astrophys. 609, A59. https://doi.org/10.1051/0004-6361/201731524.

Boroson, D.M., Robinson, B.S., 2014. The lunar laser communication demonstration: NASA’s first step toward very high data rate support of science and exploration missions. Space Sci. Rev. 185 (1–4), 115–128. https://doi.org/10.1007/s11214-014-0122-y.

Bowen, J., Tsuda, A., Abel, J., et al., 2015. CubeSat Proximity Operations Demonstration (CPOD) Mission Update. In: IEEE Aerospace Conference, pp. 1–8. https://doi.org/10.1109/AERO.2015.7119124.

Brashears, T.R., 2024. Achieving 99% link uptime on a fleet of 100G space laser inter-satellite links in LEO. In: Hemmati, H., Robinson, B.S. (Eds.), Free-Space Laser Communications XXXVI (p. 1287702). International Society for Optics and Photonics SPIE volume 12877. doi:10.1117/12.3005057.

Buinhas, L., Philips-Blum, M., Frankl, K., et al., 2018. Formation operations and navigation concept overview for the IRASSI space interferometer. In: 2018 IEEE Aerospace Conference, pp. 1–16. https://doi.org/10.1109/AERO.2018.8396827.

Burch, J.L., Moore, T.E., Torbert, R.B., et al., 2016. Magnetospheric multiscale overview and science objectives. Space Sci. Rev. 199 (1), 5–21. https://doi.org/10.1007/s11214-015-0164-9.

Cahoy, K., Grenfell, P., Crews, A., et al., 2018. The CubeSat Laser Infrared CrosslinK Mission (CLICK). https://doi.org/10.1117/12.2535953.

Chaudhry, A.U., Yanikomeroglu, H., 2021. Laser intersatellite links in a starlink constellation: a classification and analysis. IEEE Veh. Technol. Mag. 16 (2), 48–56. https://doi.org/10.1109/MVT.2021.3063706.

Conrad, A.V., Axelrad, P., Haines, B., et al., 2023. Improved GPS-Based Single-Frequency Orbit Determination for the CYGNSS Spacecraft

Using GipsyX. Navigation. J. Inst. Navig. 70 (1). https://doi.org/10.33012/navi.565.
D'Angelo, P., Fernández, A., Guardabrazo, T., et al., 2012. Enhancement of GNSS navigation function by the use of Inter-Satellite Links. In: 2012 6th ESA Workshop on Satellite Navigation Technologies (Navitec 2012) & European Workshop on GNSS Signals and Signal Processing, pp. 1–6. https://doi.org/10.1109/NAVITEC.2012.6423113.
Darbeheshti, N., Wegener, H., Müller, V., et al., 2017. Instrument data simulations for GRACE Follow-on: observation and noise models. Earth Syst. Sci. Data 9 (2), 833–848. https://doi.org/10.5194/essd-9-833-2017.
Davis, B., Gunter, B.C., 2022. Improvement of constellation orbit determination through the incorporation of intersatellite ranging. J. Guid., Control, Dynam. 45 (12), 2403–2410. https://doi.org/10.2514/1.G006566.
De Kok, M., Velazco, J., Bentum, M., 2020. CubeSat Array for Detection of RF emissions from exoplanets using inter-satellite optical communicators. In: IEEE Aerospace Conference Proceedings. IEEE Computer Society. https://doi.org/10.1109/AERO47225.2020.9172296.
Degnan, J., 1985. Satellite laser ranging: current status and future prospects. IEEE Trans. Geosci. Remote Sens. GE-23 (4), 398–413. https://doi.org/10.1109/tgrs.1985.289430.
Degnan, J., 1994. Satellite Laser Ranging in the 1990s: Report of the 1994 Belmont Workshop. In Workshop held at the Belmont Conference Center, URL: https://ntrs.nasa.gov/citations/19950007860.
Dekens, E., Engelen, S., Noomen, R., 2013. A satellite swarm for radio astronomy. Acta Astronaut. 102, 321–331. https://doi.org/10.1016/j.actaastro.2013.11.033.
Di Benedetto, M., Imperi, L., Durante, D., et al., 2019. Augmenting NASA Europa Clipper by a small probe: Europa Tomography Probe (ETP) mission concept. Acta Astronaut. 165, 211–218. https://doi.org/10.1016/j.actaastro.2019.07.027.
Dirkx, D., 2015. Interplanetary Laser Ranging: Analysis for implementation in planetary science missions. Phd thesis Delft University of Technology. URL: http://resolver.tudelft.nl/uuid:bd728e02-f403-4cea-9e2b-65b04b47b3f7.
Dirkx, D., Noomen, R., Visser, P.N.A.M., et al., 2015. Comparative analysis of one- and two-way planetary laser ranging concepts. Planet. Space Sci. 117, 159–176. https://doi.org/10.1016/j.pss.2015.06.005.
Dirkx, D., Prochazka, I., Bauer, S., et al., 2019. Laser and radio tracking for planetary science missions—a comparison. J. Geodesy 93 (11), 2405–2420. https://doi.org/10.1007/s00190-018-1171-x.
ESA, 2004. XEUS CDF REPORT. Report ESA. URL: https://sci.esa.int/documents/34923/36148/1567255369846-XEUS_CDF_Report.pdf.
ESA Earth and Mission Science Division (2020). Next generation gravity mission as a mass change and geosciences international constellation (MAGIC) a joint ESA/NASA double-pair mission based on NASA's MCDO and ESA's NGGM studies- Mission Requirements Document. Report ESA-EOPSM-FMCC-MRD-3785 European Space Research and Technology Centre. URL: https://esamultimedia.esa.int/docs/EarthObservation/MAGIC_NGGM_MCDO_MRD_v1_0-signed2.pdf.
Esteban, J.J., García, A.F., Barke, S., et al., 2011. Experimental demonstration of weak-light laser ranging and data communication for LISA. Opt. Exp. 19 (17), 15937–15946. https://doi.org/10.1364/OE.19.015937.
Evangelista, Y., Fiore, F., Fuschino, F., et al., 2020. The scientific payload on-board the HERMES-TP and HERMES-SP CubeSat missions. In: den Herder, J.W.A., Nikzad, S., Nakazawa, K. (Eds.), Proceedings of SPIE - The International Society for Optical Engineering. SPIE volume 11444. https://doi.org/10.1117/12.2561018.
Eyer, J.K., Damaren, C.J., Zee, R.E., et al., 2007. A formation flying control algorithms for the CanX-4&5 low earth orbit nanosatellite mission. Space Technol. 27 (4), 147–158, URL: https://www.scopus.com/inward/record.uri?eid=2-s2.0-44349157039&partnerID=40&md5=144a70d7f6abf8de99fc9f70080fa2ec.
Farahmand, M., Long, A., Hollister, J., et al., 2017. Magnetospheric multiscale mission navigation performance during apogee-raising and beyond. In: AAS/AIAA Astrodynamics Specialist Conference.
Fausch, R.G., Moeller, G., Rothacher, M., et al., 2022. CHESS: measuring the dynamics of composition and density of Earth's Upper Atmosphere with CubeSats. In: IEEE Aerospace Conference Proceedings. IEEE Computer Society volume 2022-March. https://doi.org/10.1109/AERO53065.2022.9843791.
Fermi, M., Gregnanin, M., Mazzolena, M., et al., 2010. The lunar gravity mission MAGIA: Preliminary design and performances. Exp. Astron. 32 (1), 1–18. https://doi.org/10.1007/s10686-010-9188-z.
Fiore, F., Burderi, L., Lavagna, M., et al., 2020. The HERMES-technologic and scientific pathfinder. In: den Herder, J.W.A., Nikzad, S., Nakazawa, K. (Eds.), Proceedings of SPIE - The International Society for Optical Engineering. SPIE volume 11444. https://doi.org/10.1117/12.2560680.
Flechtner, F., Reigber, C., Rummel, R., et al., 2021. Satellite gravimetry: a review of its realization. Surv. Geophys. 42 (5), 1029–1074. https://doi.org/10.1007/s10712-021-09658-0.
Floberghagen, R., Fehringer, M., Lamarre, D., et al., 2011. Mission design, operation and exploitation of the gravity field and steady-state ocean circulation explorer mission. J. Geodesy 85 (11), 749–758. https://doi.org/10.1007/s00190-011-0498-3.
Friis-Christensen, E., Lühr, H., Hulot, G., 2006. Swarm: A constellation to study the Earth's magnetic field. Earth, Planets and Space 58 (4), 351–358. https://doi.org/10.1186/bf03351933.
Garattini, M., Lops, C., Dell'Agnello, S., et al., 2012. Probing gravity with the proposed MAGIA and ILN lunar missions. Memorie della Societa Astron. Italiana 83, 382, URL: https://articles.adsabs.harvard.edu/-full/2012MmSAI.83.382G.
Gill, E.K.A., Steckling, M., Butz, P., 2001. Gemini: a milestone toward autonomous formation flying. In: ESA Workshop on On-Board Autonomy.
Ghobadi-Far, K., Han, S., McCullough, C.M., et al., 2020. GRACE Follow-On Laser Ranging Interferometer Measurements Uniquely Distinguish Short-Wavelength Gravitational Perturbations. Geophys. Res. Lett. 47 (16). https://doi.org/10.1029/2020gl089445.
Gill, E., D'Amico, S., Montenbruck, O., 2007. Autonomous Formation Flying for the PRISMA Mission. J. Spacecr. Rockets 44 (3), 671–681. https://doi.org/10.2514/1.23015.
Giorgi, G., Schmidt, T.D., Trainotti, C., et al., 2019. Advanced technologies for satellite navigation and geodesy. Adv. Space Res. 64 (6), 1256–1273. https://doi.org/10.1016/j.asr.2019.06.010.
Goldstein, A., Veres, P., Burns, E., et al., 2017. An ordinary short gamma-ray burst with extraordinary implications: Fermi-GBM Detection of GRB 170817A. Astrophys. J. Lett. 848 (2), L14. https://doi.org/10.3847/2041-8213/aa8f41.
Gramigna, E., Johansen, J.G., Manghi, R.L., et al., 2022. Hera inter-satellite link doppler characterization for didymos gravity science experiments. In: 2022 IEEE 9th International Workshop on Metrology for AeroSpace (MetroAeroSpace), pp. 430–435. https://doi.org/10.1109/MetroAeroSpace54187.2022.9856049.
Gramigna, E., Lasagni Manghi, R., Zannoni, M., et al., 2024. The Hera radio science experiment at didymos. Planet. Space Sci. 246, 105906. https://doi.org/10.1016/j.pss.2024.105906.
Grenfell, P., 2024. Systems Performance Analysis for Autonomous Spacecraft Navigation within Satellite Constellations using Intersatellite Optical Communications Links. Phd thesis Massachusetts Institute of Technology. URL: https://hdl.handle.net/1721.1/153778.
Haagmans, R., Siemes, C., Massotti, L., et al., 2020. ESA's next-generation gravity mission concepts. Rendiconti Lincei. Scienze Fisiche e Naturali 31 (S1), 15–25. https://doi.org/10.1007/s12210-020-00875-0.
Hamkins, J., Kinman, P., Xie, H., et al., 2015. Telemetry ranging: concepts. Interplanet. Network Prog. Rep. 42–203, 1–20, URL: https://ui.adsabs.harvard.edu/abs/2015IPNPR.203C...1H.
Hamkins, J., Kinman, P., Xu, Z., et al., 2016a. Telemetry ranging: laboratory validation tests and end-to-end performance. IPN Prog.

Rep., 42–206, URL: https://uiadsabs.harvard.edu/abs/2016IPNPR.206D...1H.
Hamkins, J., Kinmany, P., Xie, H. et al., 2016b. Telemetry Ranging: Signal Processing. Interplanetary Network Progress Report, (pp. 42–204). URL: https://ui.adsabs.harvard.edu/abs/2016IPNPR.204D...1H.
Heinzel, G., Sheard, B., Brause, N., et al., 2017. Laser ranging interferometer for GRACE follow-on. In: Armandillo, E., Cugny, B., Karafolas, N. (Eds.), Proceedings of SPIE - The International Society for Optical Engineering. SPIE volume 10564. https://doi.org/10.1117/12.2309099.
Henkel, P., 2020. Precise Point Positioning for Next-Generation GNSS. In: European Navigation Conference (ENC), pp. 1–11. https://doi.org/10.23919/ENC48637.2020.9317475.
Hoffman, T.L., 2009. GRAIL: Gravity mapping the moon. IEEE Aerospace Conference Proceedings. https://doi.org/10.1109/AERO.2009.4839327.
Huyan, Z., Zhu, J., Wang, Y. et al., 2020. Initial Results of BDS3 GEO Orbit Determination with Inter-satellite Link Measurements. In: China Satellite Navigation Conference (CSNC) 2020 Proceedings: Volume II Lecture Notes in Electrical Engineering book section Chapter 7. (pp. 71–82). doi:10.1007/978-981-15-3711-0_7.
van den Ijssel, J., Encarnação, J., Doornbos, E., et al., 2015. Precise science orbits for the Swarm satellite constellation. Adv. Space Res. 56 (6), 1042–1055. https://doi.org/10.1016/j.asr.2015.06.002.
Jones, D.L., Allen, R., Basart, J., et al., 2000. The astronomical low frequency array: A proposed explorer mission for radio astronomy. In: Stone, R.G., Bougeret, J.L., Goldstein, M.L., et al. (Eds.), Geophys. Monogr. Ser., volume 119. Blackwell Publishing Ltd, pp. 339–349. https://doi.org/10.1029/GM119p0339.
Jäggi, A., Montenbruck, O., Moon, Y., et al., 2012. Inter-agency comparison of TanDEM-X baseline solutions. Adv. Space Res. 50 (2), 260–271. https://doi.org/10.1016/j.asr.2012.03.027.
Karunanithi, V., Rajan, R.T., Sundaramoorthy, P. et al., 2019. High data-rate inter-satellite link (ISL) for space-based interferometry. In: 70th International Astronautical Congress, IAC 2019. volume 2019-October of Proceedings of the International Astronautical Congress, IAC. URL: https://research.tudelft.nl/files/67473541/IAC_2019_OLFAR_COMM_v1.3.pdf.
Kaushal, H., Kaddoum, G., 2017. Optical communication in space: challenges and mitigation techniques. IEEE Commun. Surv. Tutor. 19 (1), 57–96. https://doi.org/10.1109/comst.2016.2603518.
Kim, J., 2000. Simulation Study of a Low-Low Satellite-to-Satellite Tracking Mission. Phd thesis The University of Texas at Austin. URL: https://granite.phys.s.u-tokyo.ac.jp/ando/GRACE/Kim_dissertation.pdf.
Kim, J., Lee, S.W., 2009. Flight performance analysis of GRACE K-band ranging instrument with simulation data. Acta Astronaut. 65 (11–12), 1571–1581. https://doi.org/10.1016/j.actaastro.2009.04.010.
Kim, W., Fu, H., Lee, K., et al., 2020. Photonic microwave distance interferometry using a mode-locked laser with systematic error correction. Appl. Sci. 10 (21). https://doi.org/10.3390/app10217649.
Klein, K.G., Spence, H., Alexandrova, O., et al., 2023. HelioSwarm: A Multipoint, Multiscale Mission to Characterize Turbulence. Space Sci. Rev. 219 (8), 74. https://doi.org/10.1007/s11214-023-01019-0.
Klipstein, W.M., Arnold, B.W., Enzer, D.G., et al., 2013. The lunar gravity ranging system for the Gravity Recovery and Interior Laboratory (GRAIL) mission. Space Sci. Rev. 178 (1), 57–76. https://doi.org/10.1007/s11214-013-9973-x.
Knapp, M., Babuscia, A., Jensen-Clem, R. et al., 2013. SOLARA/SARA: Solar Observing Low-frequency Array for Radio Astronomy/Separated Antennas Reconfigurable Array. In: Sandau, R., Nakasuka, S., Kawashima, R., et al. (Eds.), Innovative Ideas for Micro/Nano-Satellite Missions (pp. 2–15). International Academy of Astronautics (IAA). URL: https://www.songsofexoplanets.com/publications/17724.pdf.
Konopliv, A.S., Park, R.S., Yuan, D.-N., et al., 2013. The JPL lunar gravity field to spherical harmonic degree 660 from the GRAIL Primary Mission. J. Geophys. Res.: Planets 118 (7), 1415–1434. https://doi.org/10.1002/jgre.20097.
Li, W., Cardellach, E., Fabra, F., et al., 2020. Assessment of Spaceborne GNSS-R Ocean Altimetry Performance Using CYGNSS Mission Raw Data. IEEE Trans. Geosci. Remote Sens. 58 (1), 238–250. https://doi.org/10.1109/TGRS.2019.2936108.
Li, X., Jiang, Z., Ma, F., et al., 2019. LEO precise orbit determination with inter-satellite links. Remote Sens. 11 (18). https://doi.org/10.3390/rs11182117.
Li, X., Wu, W., Guo, J., et al., 2013. The method and development trend of laser ranging. In: 2013 5th International Conference on Intelligent Human-Machine Systems and Cybernetics, pp. 7–10. https://doi.org/10.1109/ihmsc.2013.149.
Linz, H., Bhatia, D., Buinhas, L., et al., 2020. InfraRed Astronomy Satellite Swarm Interferometry (IRASSI): Overview and study results. Adv. Space Res. 65 (2), 831–849. https://doi.org/10.1016/j.asr.2019.06.022.
Llorente, J.S., Agenjo, A., Carrascosa, C., de Negueruela, C., Mestreau-Garreau, A., Cropp, A., 2013. PROBA-3: Precise formation flying demonstration mission. Acta Astronaut. 82, 38–46. https://doi.org/10.1016/j.actaastro.2012.05.029.
Long, A., Farahmand, M., Carpenter, R., 2015. Navigation operations for the magnetospheric multiscale mission. In: International Symposium on Space Flight Dynamics.
Luo, Z., Wang, Y., Wu, Y., et al., 2021. The Taiji program: a concise overview. Prog. Theoret. Exp. Phys. 2021 (5). https://doi.org/10.1093/ptep/ptaa083.
Lv, Y., Geng, T., Zhao, Q., et al., 2020. Evaluation of BDS-3 orbit determination strategies using ground-tracking and inter-satellite link observation. Remote Sens. 12 (16). https://doi.org/10.3390/rs12162647.
MacDowall, R.J., Bale, S.D., Demaio, L. et al., 2005. Solar Imaging Radio Array (SIRA): A multi-spacecraft mission. In: Proceedings of SPIE - The International Society for Optical Engineering, pp. 284–292. volume 5659. doi:10.1117/12.578736.
Mao, X., Visser, P.N.A.M., van den Ijssel, J., 2019. High-dynamic baseline determination for the Swarm constellation. Aerosp. Sci. Technol. 88, 329–339. https://doi.org/10.1016/j.ast.2019.03.031.
Marcos, B., David, H.L., Anthony, J.P., 2004. XEUS mission reference design. In: Proc.SPIE, pp. 530–538. volume 5488. doi:10.1117/12.552928.
Marz, S., Schlicht, A., Hugentobler, U., 2021. Galileo precise orbit determination with optical two-way links (OTWL): a continuous wave laser ranging and time transfer concept. J. Geodesy 95 (7). https://doi.org/10.1007/s00190-021-01534-4.
Mei, J., Bai, Y.-Z., Bao, J., et al., 2021. The TianQin project: current progress on science and technology. Prog. Theoret. Exp. Phys. 2021 (5). https://doi.org/10.1093/ptep/ptaa114.
Melman, F.T., Zoccarato, P., Orgel, C., et al., 2022. LCNS positioning of a lunar surface rover using a DEM-Based Altitude Constraint. Remote Sens. 14 (16). https://doi.org/10.3390/rs14163942.
Ming, M., Luo, Y., Liang, Y.-R., et al., 2020. Ultraprecision intersatellite laser interferometry. Int. J. Extreme Manuf. 2 (2). https://doi.org/10.1088/2631-7990/ab8864.
Montenbruck, O., Gill, E., 2000. Satellite Orbits: Models, Methods and Applications. Springer, Berlin, Heidelberg. https://doi.org/10.1007/978-3-642-58351-3.
Montenbruck, O., Hackel, S., Van Den Ijssel, J., et al., 2018. Reduced dynamic and kinematic precise orbit determination for the Swarm mission from 4 years of GPS tracking. GPS Solut. 22 (3). https://doi.org/10.1007/s10291-018-0746-6.
Moreira, A., Krieger, G., Hajnsek, I. et al., 2015. Tandem-L/ALOSNext: A Highly Innovative Bistatic SAR Mission for Global Observation of Dynamic Processes on the Earth's Surface. IEEE Geosc Remote Sens Mag 3 (2): 8–23. IEEE Geoscience Remote Sensing Magazine, 3(2). doi:10.1109/MGRS.2015.2437353.

Musha, M., 2017. Space gravitational wave antenna DECIGO and B-DECIGO. CEAS Space J. 9 (4), 371–377. https://doi.org/10.1007/s12567-017-0177-1.

Musha, M., Tajiri, M., Akami, K., et al., 2021. Laser-based satellite positioning system for space gravitational wave detector DECIGO. https://doi.org/10.1117/12.2599634.

Net, M.S., 2023. Optical ranging: asynchronous-mode concept, prototype and validation. Interplanet. Network Prog. Rep. 42–232, 1–18, URL: https://ipnpr.jpl.nasa.gov/progress_report/42-232/42-232A.pdf.

Net, M.S., Hamkins, J., 2020. Optical Telemetry Ranging. The Interplanetary Network Progress Report,. URL: https://ipnpr.jpl.nasa.gov/progress_report/42-221/42-221B.pdf.

Notaro, V., Di Benedetto, M., Colasurdo, G., et al., 2020. A small spacecraft to probe the interior of the Jovian moon Europa: Europa Tomography Probe (ETP) system design. Acta Astronaut. 166, 137–146. https://doi.org/10.1016/j.actaastro.2019.10.017.

Oberoi, D., Pinçon, J.-L., 2005. A new design for a very low frequency spaceborne radio interferometer. Radio Sci. 40 (4). https://doi.org/10.1029/2004RS003211.

Oudrhiri, K., Asmar, S., Esterhuizen, S., et al., 2014. An innovative direct measurement of the GRAIL absolute timing of Science Data. In: IEEE Aerospace Conference Proceedings. IEEE Computer Society. https://doi.org/10.1109/AERO.2014.6836453.

Pail, R., Bamber, J., Biancale, R., et al., 2019. Mass variation observing system by high low inter-satellite links (MOBILE) – a new concept for sustained observation of mass transport from space. J. Geodetic Sci. 9 (1), 48–58. https://doi.org/10.1515/jogs-2019-0006.

Perrotta, G., Stipa, M., Silvi, D., et al., 2010. Mission-constrained design drivers and technical solutions for the MAGIA satellite. Exp. Astron. 32 (1), 63–82. https://doi.org/10.1007/s10686-010-9209-y.

Persson, S., Jacobsson, B., Gill, E., 2005. Prisma - Demonstration mission for advanced rendezvous and formation flying technologies and sensors. In International Astronautical Federation - 56th International Astronautical Congress 2005 (pp. 2403–2412). volume 4. doi:10.2514/6.Iac-05-b5.6.B.07.

Peter J.G. Teunissen, Oliver Montenbruck (Ed.) (2017). Springer Handbook of Global Navigation Satellite Systems volume XXXI. Springer. URL: http://www.springer.com/gp/book/9783319429267.

Persson, S., Bodin, P., Gill, E., et al., 2006. PRISMA - An autonomous formation flying mission. In: European Space Agency, (Special Publication) ESA SP. volume 625 SP, URL: https://www.dlr.de/de/rb/importiert-aus-cxxl/gsoc_dokumente/rb-rft/ESA4S_06_10a.pdf.

Plice, L., Perez, A.D., West, S., 2019. Helioswarm: Swarm mission design in high altitude orbit for heliophysics. In: Horneman, K.R., Scott, C., Hansen, B.W., et al. (Eds.), Advances in the Astronautical Sciences, volume 171. Univelt Inc., pp. 1787–1804, URL: https://ntrs.nasa.gov/citations/20190029108.

Policastri, L., Woodburn, J., 2019. Helioswarm: Space-based relative ranging for a cubesat cluster mission in a 2:1 lunar resonant orbit. In: Horneman, K.R., Scott, C., Hansen, B.W., et al. (Eds.), Advances in the Astronautical Sciences, volume 171. Univelt Inc., pp. 565–576, URL: https://ntrs.nasa.gov/api/citations/20190029108/downloads/20190029108.pdf.

Reigber, C., Schwintzer, P., Lühr, H., et al., 1999. The champ geopotential mission. Boll. Geof. Teor. Appl 40 (3–4), 285–289.

Rivkin, A.S., Cheng, A.F., 2023. Planetary defense with the Double Asteroid Redirection Test (DART) mission and prospects. Nat. Commun. 14 (1). https://doi.org/10.1038/s41467-022-35561-2.

Ruf, C.S., Gleason, S., Jelenak, Z. et al., 2012. The CYGNSS nanosatellite constellation hurricane mission. In: 2012 IEEE International Geoscience and Remote Sensing Symposium, pp. 214–216. doi:10.1109/IGARSS.2012.6351600.

Sanna, A., Burderi, L., Di Salvo, T. et al., 2020. Timing techniques applied to distributed modular high-energy astronomy: the H.E.R.M.E.S. project. In J.-W.A. den Herder, S. Nikzad, & K. Nakazawa (Eds.), Space Telescopes and Instrumentation 2020: Ultraviolet to Gamma Ray (p. 114444X). volume 11444. doi:10.1117/12.2561758.

Savchenko, V., Ferrigno, C., Kuulkers, E., et al., 2017. INTEGRAL Detection of the First Prompt Gamma-Ray Signal Coincident with the Gravitational-wave Event GW170817. Astrophys. J. Lett. 848 (2), L15. https://doi.org/10.3847/2041-8213/aa8f94.

Schieler, C., Riesing, K., Horvath, A., et al., 2022. In: Hemmati, H., Robinson, B.S. (Eds.), In: Free-Space Laser Communications XXXIV, 119930. SPIE. https://doi.org/10.1117/12.2615321.

Seto, N., Kawamura, S., Nakamura, T., 2001. Possibility of Direct Measurement of the Acceleration of the Universe Using 0.1 Hz Band Laser Interferometer Gravitational Wave Antenna in Space. Phys. Rev. Lett. 87 (22), 221103. https://doi.org/10.1103/PhysRevLett.87.221103.

Sheard, B.S., Heinzel, G., Danzmann, K., et al., 2012. Intersatellite laser ranging instrument for the GRACE follow-on mission. J. Geodesy 86 (12), 1083–1095. https://doi.org/10.1007/s00190-012-0566-3.

Serra, P.C.,Tomio, H., Cierny, O. et al., 2021. CubeSat laser infrared crosslinK mission status. In: Cugny, B., Sodnik, Z., Karafolas, N. (Eds.), International Conference on Space Optics — ICSO 2021. SPIE volume 11852. doi:10.1117/12.2599543.

Smith, D.E., Zuber, M.T., Mazarico, E., et al., 2018. Trilogy, a planetary geodesy mission concept for measuring the expansion of the solar system. Planet. Space Sci. 153, 127–133. https://doi.org/10.1016/j.pss.2018.02.003.

Sodnik, Z., Furch, B., Lutz, H., 2010. Optical Intersatellite Communication. IEEE J. Sel. Top. Quantum Electron. 16 (5), 1051–1057. https://doi.org/10.1109/jstqe.2010.2047383.

Singh, U.K., Shankar, M.R.B., Ottersten, B., 2022. Opportunistic localization using LEO signals. In: 2022 56th Asilomar Conference on Signals, Systems, and Computers, pp. 894–899. doi:10.1109/IEEECONF56349.2022.10051941.

Spring-Turner, C., Thilak Rajan, R., 2022. Performance Bounds for Cooperative Localisation in the Starlink Network. arXiv e-prints, (p. arXiv:2207.04691). doi:10.48550/arXiv.2207.04691. arXiv:2207.04691.

Stevens, M.L., Parenti, R.R., Willis, M.M., et al., 2016. The lunar laser communication demonstration time-of-flight measurement system: overview, on-orbit performance, and ranging analysis. Free-Space Laser Communication and Atmospheric Propagation XXVIII. https://doi.org/10.1117/12.2218624.

Tapley, B.D., 2008. Gravity model determination from the GRACE mission. J. Astronaut. Sci. 56 (3), 273–285. https://doi.org/10.1007/BF03256553.

Tolker-Nielsen, T., & Oppenhauser, G., 2002. In-orbit test result of an operational optical intersatellite link between ARTEMIS and SPOT4, SILEX. In: Free-Space Laser Communication Technologies XIV, pp. 1–15. doi:10.1117/12.464105.

Tomio, H., Grenfell, P., Kammerer, W. et al., 2022. Development and Testing of the Laser Transmitter and Pointing, Acquisition, and Tracking System for the CubeSat Laser Infrared CrosslinK (CLICK) B/C Mission. doi:10.1109/icsos53063.2022.9749715.

Toyoshima, M., 2021. Recent trends in space laser communications for small satellites and constellations. J. Lightwave Technol. 39 (3), 693–699.

Turan, E., Speretta, S., Gill, E., 2022. Autonomous navigation performance of cislunar orbits considering high crosslink measurement errors. https://doi.org/10.1109/aero53065.2022.9843772.

Turan, E., Speretta, S., Gill, E., 2023. Performance analysis of crosslink radiometric measurement based autonomous orbit determination for cislunar small satellite formations. Adv. Space Res. 72 (7), 2710–2732. https://doi.org/10.1016/j.asr.2022.11.032.

Turyshev, S.G., Toth, V.T., Sazhin, M.V., 2013. General relativistic observables of the grail mission. Phys. Rev. D 87 (2). https://doi.org/10.1103/physrevd.87.024020.

Velazco, J., 2023a. Cislunar omnidirectional optical terminal for fast connectivity and accurate navigation. In: 2023 IEEE Aerospace Conference (pp. 1–7). doi:10.1109/AERO55745.2023.10115660.

Velazco, J., 2023b. INSPIRE - A Connectivity Network for the Solar System. In: 2023 IEEE Aerospace Conference (pp. 1–13). doi:10.1109/AERO55745.2023.10115844.

Velazco, J.E., Aguilar, A., Klaib, A.R., et al., 2020. Development of omnidirectional optical terminals for swarm communications and navigation. Interplanet. Network Prog. Rep., 42–221, 1–8, URL: https://ipnpr.jpl.nasa.gov/progress_report/42-221/42-221A.pdf.

Velazco, J.E., Vega, J.S. d. l., 2020. Q4 – A CubeSat Mission to Demonstrate Omnidirectional Optical Communications. In: 2020 IEEE Aerospace Conference (pp. 1–6). doi:10.1109/AERO47225.2020.9172329.

Vilnrotter, V., Hamkins, J., 2019. Telecommand/telemetry ranging for deep-space applications. In: IEEE Aerospace Conference (pp. 1–10). doi:10.1109/AERO.2019.8742212.

Werner, N., Rípa, J., Pál, A. et al., 2018. CAMELOT: Cubesats Applied for MEasuring and LOcalising Transients mission overview. In: S. Nikzad, J.W.A. Den Herder, & K. Nakazawa (Eds.), Proceedings of SPIE - The International Society for Optical Engineering. SPIE volume 10699. doi:10.1117/12.2313764.

Wiese, D.N., Bienstock, B., Blackwood, C., et al., 2022. The mass change designated observable study: overview and results. Earth Space Sci. 9 (8). https://doi.org/10.1029/2022ea002311.

Winternitz, L.B., Bamford, W.A., Price, S.R., 2017a. New high-altitude GPS navigation results from the magnetospheric multiscale spacecraft and simulations at Lunar distances. In: 30th International Technical Meeting of the Satellite Division of the Institute of Navigation, ION GNSS 2017 (pp. 1114–1126). Institute of Navigation volume 2. doi:10.33012/2017.15367.

Winternitz, L.B., Bamford, W.A., Price, S.R., et al., 2017b. Global Positioning System Navigation Above 76,000 km for NASA'S Magnetospheric Multiscale Mission. Navigation 64 (2), 289–300. https://doi.org/10.1002/navi.198.

Wishart, A., Teston, F., Kemble, S. et al., 2007. The PROBA-3 formation flying technology demonstration mission. In International Astronautical Federation - 58th International Astronautical Congress 2007 (pp. 4551–4561). volume 7.

Xie, X., Geng, T., Zhao, Q., et al., 2020. Orbit and clock analysis of BDS-3 satellites using inter-satellite link observations. J. Geodesy 94 (7). https://doi.org/10.1007/s00190-020-01394-4.

Yao, X., Ren, S., Zhang, Z. et al. (2021). Inter-satellite laser ranging for time-delay interferometry in space-based gravitational-wave detection. In: Yang, Y. (Ed.), Proceedings of SPIE - The International Society for Optical Engineering. SPIE volume 12057. doi:10.1117/12.2606128.

Yared, N., Jansson, G., 2023. Telesat Lightspeed: enabling mesh network solutions for managed data service flexibility across the globe volume 12413 of SPIE LASE. SPIE, URL: https://doi.org/10.1117/12.2646211.

Zhang, J.Y., Ming, M., Jiang, Y.Z., et al., 2018. Inter-satellite laser link acquisition with dual-way scanning for Space Advanced Gravity Measurements mission. Rev Sci Instrum 89 (6), 064501. https://doi.org/10.1063/1.5019433.

Zhang, Z., Deng, L., Feng, J., et al., 2022. A Survey of Precision Formation Relative State Measurement Technology for Distributed Spacecraft. Aerospace 9 (7), 362. https://doi.org/10.3390/aerospace9070362.

Zhao, Q., Yu, L., Du, Z., et al., 2022. An overview of the applications of earth observation satellite data: impacts and future trends. Remote Sens. 14 (8). https://doi.org/10.3390/rs14081863.

Zheng, W., Li, Z., 2018. Preferred design and error analysis for the future dedicated deep-space Mars-SST satellite gravity mission. Astrophys. Space Sci. 363 (8). https://doi.org/10.1007/s10509-018-3392-0.

Zhu, J., Li, H., Li, J., et al., 2022. Performance of dual one-way measurements and precise orbit determination for BDS via inter-satellite link. Open Astron. 31 (1), 276–286. https://doi.org/10.1515/astro-2022-0034.

Zink, M., Fiedler, H., Hajnsek, I. et al., 2006. The TanDEM-X Mission Concept. In: 2006 IEEE International Symposium on Geoscience and Remote Sensing (pp. 1938–1941). doi:10.1109/IGARSS.2006.501.